



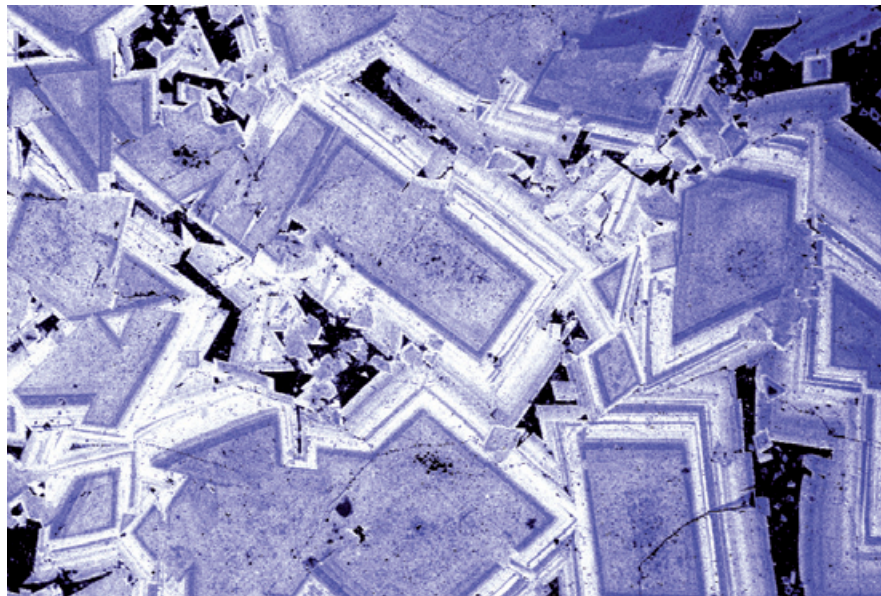
**British
Geological Survey**

NATURAL ENVIRONMENT RESEARCH COUNCIL

Stratabound Pb–Zn–Ba–F mineralisation in the Alston Block of the North Pennine Orefield (England) — origins and emplacement

Economic Minerals Programme

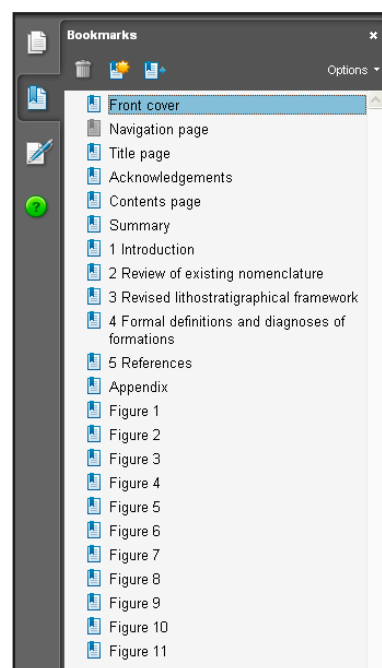
Research Report RR/08/06



HOW TO NAVIGATE THIS DOCUMENT

Bookmarks

The main elements of the table of contents are bookmarked enabling direct links to be followed to the principal section headings and sub-headings, figures, plates and tables irrespective of which part of the document the user is viewing.



In addition, the report contains links:



from the principal section and subsection headings back to the contents page,



from each reference to a figure, plate or table directly to the corresponding figure, plate or table,



from each figure, plate or table caption to the first place that figure, plate or table is mentioned in the text and



from each page number back to the contents page.

[RETURN TO CONTENTS PAGE](#)

The National Grid and other Ordnance Survey data are used with the permission of the Controller of Her Majesty's Stationery Office.
Licence No: 100017897/2008.

ISBN 978 0 85272 625 9

Front cover

Scanning electron microscope image showing well-developed compositional zoning in wall-rock replacive dolomite, Small Cleugh Mine, Nenthead.

Bibliographical reference

BOUCH, J E, NADEN, J, SHEPHERD, T J, YOUNG, B, BENHAM, A J, MCKERVEY, J A, SLOANE, H J. 2008. Stratabound Pb-Zn-Ba-F mineralisation in the Alston Block of the North Pennine Orefield (England) — origins and emplacement. *British Geological Survey Research Report*, RR/08/06.

Copyright in materials derived from the British Geological Survey's work is owned by the Natural Environment Research Council (NERC) and/or the authority that commissioned the work. You may not copy or adapt this publication without first obtaining permission. Contact the BGS Intellectual Property Rights Section, British Geological Survey, Keyworth, e-mail ipr@bgs.ac.uk. You may quote extracts of a reasonable length without prior permission, provided a full acknowledgement is given of the source of the extract.

Your use of any information provided by the British Geological Survey (BGS) is at your own risk. Neither BGS nor the Natural Environment Research Council gives any warranty, condition or representation as to the quality, accuracy or completeness of the information or its suitability for any use or purpose. All implied conditions relating to the quality or suitability of the information, and all liabilities arising from the supply of the information (including any liability arising in negligence) are excluded to the fullest extent permitted by law.

Stratabound Pb–Zn–Ba–F mineralisation in the Alston Block of the North Pennine Orefield (England) — origins and emplacement

J E Bouch^{1*}, J Naden¹, T J Shepherd², B Young³, A J Benham¹, J A McKervey¹, H J Sloane⁴

- 1 British Geological Survey, Keyworth, Nottingham
- 2 School of Earth Sciences, University of Leeds
- 3 British Geological Survey, Murchison House, Edinburgh
- 4 Natural Environment Research Council Isotope Geosciences Laboratory, Keyworth, Nottingham

BRITISH GEOLOGICAL SURVEY

The full range of our publications is available from BGS shops at Nottingham, Edinburgh, London and Cardiff (Welsh publications only) see contact details below or shop online at www.geologyshop.com

The London Information Office also maintains a reference collection of BGS publications, including maps, for consultation.

We publish an annual catalogue of our maps and other publications; this catalogue is available online or from any of the BGS shops.

The British Geological Survey carries out the geological survey of Great Britain and Northern Ireland (the latter as an agency service for the government of Northern Ireland), and of the surrounding continental shelf, as well as basic research projects. It also undertakes programmes of technical aid in geology in developing countries.

The British Geological Survey is a component body of the Natural Environment Research Council.

British Geological Survey offices

BGS Central Enquiries Desk

Tel 0115 936 3143 Fax 0115 936 3276
email enquires@bgs.ac.uk

Kingsley Dunham Centre, Keyworth, Nottingham NG12 5GG

Tel 0115 936 3241 Fax 0115 936 3488
email sales@bgs.ac.uk

Murchison House, West Mains Road, Edinburgh EH9 3LA

Tel 0131 667 1000 Fax 0131 668 2683
email scotsales@bgs.ac.uk

London Information Office at the Natural History Museum (Earth Galleries), Exhibition Road, South Kensington, London SW7 2DE

Tel 020 7589 4090 Fax 020 7584 8270
Tel 020 7942 5344/45 email bgs-london@bgs.ac.uk

Columbus House, Greenmeadow Springs, Tongwynlais, Cardiff CF15 7NE

Tel 029 2052 1962 Fax 029 2052 1963

Forde House, Park Five Business Centre, Harrier Way, Sowton EX2 7HU

Tel 01392 445271 Fax 01392 445371

Maclea Building, Crowmarsh Gifford, Wallingford OX10 8BB

Tel 01491 838800 Fax 01491 692345

Geological Survey of Northern Ireland, Colby House, Stranmillis Court, Belfast BT9 5BF

Tel 028 9038 8462 Fax 028 9038 8461
www.bgs.ac.uk/gsni/

Parent Body

Natural Environment Research Council, Polaris House, North Star Avenue, Swindon SN2 1EU

Tel 01793 411500 Fax 01793 411501
www.nerc.ac.uk

Website www.bgs.ac.uk

Shop online at www.geologyshop.com

Abstract

The North Pennine Orefield Alston Block has produced approximately 4 Mt Pb, 0.3 Mt Zn, 2.1 Mt fluorite, 1.5 Mt barite, 1 Mt witherite plus a substantial amount of iron ore and copper ore from predominantly vein-hosted mineralisation in Carboniferous Limestones. However, a significant proportion of this production (c.20 per cent) came from stratabound deposits. Though much is known about the vein-mineralisation, the relationship between the veins and the stratabound mineralisation is not well understood. New petrographic, isotopic and fluid inclusion data derived from samples of stratabound mineralisation allow us to present a unified model that addresses the genesis of both the vein and stratabound styles of mineralisation. We recognise three episodes of mineralisation:

(i) **Dolomitisation and ankeritisation** — in the vicinity of the stratabound mineralisation limestones are pervasively dolomitised/ankeritised with extensively developed vuggy porosity. This occurred in the presence of a high-salinity

brine consistent with fluids derived from adjacent mud and shale-filled basins.

(ii) **Main stage fluorite–quartz–sulphide mineralisation** — in addition to metasomatic limestone replacement, repeated brecciation, dissolution and hydrothermal karstification plus additional porosity modification and redistribution of carbonate occurred, with open space filled with fluorite, galena, sphalerite, quartz and barite. Microthermometric and microchemical fluid inclusion data provide direct evidence for mineralisation in response to mixing of a low-salinity sodic groundwater with a high-salinity, calcic, Fe-rich, metalliferous brine which had highly elevated metal contents relative to ‘normal’ high total dissolved sulphur (TDS) sedimentary brines.

(iii) **Late stage barite mineralisation** — this is paragenetically late and appears to represent the waning stages or distal portions of the main hydrothermal circulation under cooler conditions.

Acknowledgements

The authors wish to thank numerous colleagues who have provided valuable technical support throughout this study. David Banks and Linda Berry, University of Leeds, are

thanked for assistance given to BGS during setting up of the laser ablation system for the fluid inclusion microchemical analyses.

Contents

1 Introduction	1
1.1 Geological setting	2
1.2 Stratabound mineralisation in the North Pennine Orefield	2
1.3 Materials and methods	4
2 Results	5
2.1 Site descriptions	5
2.2 Styles of stratabound mineralisation	7
2.3 Petrography, fluid inclusion microthermometry and mineral chemistry	7
2.3.1 Limestone texture and diagenesis	7
2.3.2 Anhydrite and Gypsum	8
2.3.3 Dolomite	8
2.3.4 Ankerite	8
2.3.5 Fluorite	12
2.3.6 Quartz	15
2.3.7 Sulphides	16
2.3.8 Calcite	16
2.3.9 Barite	16
2.3.10 Late carbonates	16
3 Discussion	17
3.1 Mechanisms of porosity generation	17
3.2 History of mineralisation	18
3.2.1 Burial diagenesis	18
3.2.2 Vuggy porosity generation and dolomitisation/ankeritisation	18
3.2.3 Fluorite-quartz-sulphide mineralisation	21
3.2.4 Barite mineralisation	22
Conclusions	23
References	24

FIGURES

1	The location, structure and geology of the North Pennine Orefield	2
2	Generalised stratigraphy of the North Pennine Orefield, showing the stratigraphic location and distribution of the main stratabound orebodies	3
3	Mineralisation styles associated with stratabound mineralisation in the North Pennine Orefield	6
4	Summary plots showing co-variations in carbonate composition for calcite and dolomite/ankerite	9
5	Histograms of fluid inclusion microthermometric data for samples of stratabound mineralisation in the North Pennines	10
6	Cross plots showing variations in fluid inclusion salinity	12
7	Stable isotope cross plot ($\delta^{18}\text{O}$ versus $\delta^{13}\text{C}$) with analysis points grouped according to location and mineral	12
8	Photomicrographs of main ore and gangue-phases from stratabound mineralisation in the North Pennine Orefield	13
9	Compositional variations in zebra-dolomite developed during stratabound mineralisation in the North Pennine Orefield	14
10	Features of brecciation, internal sediments and mineralised vugs	19
11	Summary diagram illustrating the evolution of the North Pennine Orefield from Lower Carboniferous through to Triassic times	20–21

TABLES

1	Stable isotope data for samples from the North Pennines	11
2	Results of laser-ablation microprobe fluid inclusion microchemical analysis	15

1 Introduction

Though currently inactive, it is estimated that mining in the North Pennine Orefield (Figure 1) of the Alston Block has produced approximately 4 million tonnes (Mt) Pb, 0.3 Mt Zn, 2.1 Mt fluorite, 1.5 Mt barite, 1 Mt witherite plus a substantial amount of iron ore and a few hundred tonnes of copper ore (Dunham, 1990). The North Pennine Orefield is a fluoritic sub-type of Mississippi Valley-type deposits akin to deposits in Kentucky and Illinois in North America (Dunham, 1990; Plant et al., 1995), and is best known for its vein-style mineralisation. Previous ore genesis studies have focused on the vein-style mineralisation, which shows strong concentric zonation with a central fluorite zone and a surrounding zone characterised by barium minerals (Figure 1b). Mineralisation in the central fluorite zone, is generally regarded as having formed from hot (120–200°C) metal-rich saline brines (about 20 wt% NaCl equiv. Sawkins, 1966; Smith, 1974; Moore, 1980; Cann and Banks, 2001). Mineralisation temperatures and salinities are lower in the surrounding barium zone (less than 120°C and about 15 wt% NaCl equiv.; Cann and Banks, 2001). In addition to the vein-style mineralisation, significant orebodies were also worked from mainly limestone-hosted stratabound mineral deposits. These formed approximately 17% of all deposits worked in the orefield (Dunham, 1990) and are thought to result from metasomatic replacement adjacent to the veins. In addition to lead, zinc, fluorite, barite and witherite, the stratabound style of mineralisation also produced iron about 1.7 Mt of iron ore (Dunham, 1990). Whereas numerous studies have been carried out on the vein mineralisation, the relationship between the vein and stratabound styles has attracted comparatively little research and there is no unified genetic model.

In this contribution we demonstrate that, in addition to metasomatism, the stratabound mineralisation results from significant fracturing, brecciation, hydrothermal karstification and associated limestone dissolution both prior to and during the main mineralisation. New stable isotope ($\delta^{13}\text{C}$ and $\delta^{18}\text{O}$ on carbonates) and fluid inclusion microthermometric data show that fluid mixing plays an important role in the genesis of the stratabound mineralisation, which is cogenetic with the main vein-style mineralisation. Finally, new microchemical fluid inclusion data show that the fluids were locally highly metalliferous, and in particular iron rich. These data also support models invoking the presence of fluids from multiple sources within the system during mineralisation. This new information, in conjunction with existing data, allows us to propose a model for the genesis of the North Pennine Orefield involving the mixing of surficial waters and basinal brines. Furthermore, as brine mixing can be one of the drivers of limestone dissolution (Corbella et al., 2004) we suggest that, in the North Pennine Orefield, this process can explain the generation of porosity in addition to ore deposition.

1.1 GEOLOGICAL SETTING

Deposits of the North Pennine Orefield are located within two structural highs (the Alston and Askrigg blocks) composed of Lower Palaeozoic sediments and volcanic rocks

intruded by Caledonian granites, overlain by comparatively thin (up to around 600 m) mainly cyclothem sequences of Carboniferous limestones, sandstones, mudstones and minor thin coals (Figures 1 and 2; Dunham and Wilson, 1985; Dunham, 1990). The blocks are separated from the adjacent sedimentary basins by a series of predominantly east–west-trending faults that controlled Carboniferous sedimentation. This allowed substantially thicker, but lithologically similar, cyclothem successions (locally in excess of 5 km) to accumulate in the rapidly subsiding basins (Chadwick et al., 1995).

This report is concerned only with the deposits of the Alston Block. Here mineralisation is hosted mainly in a conjugate system of steeply-dipping normal faults, most of which exhibit a maximum displacement of only a few metres. There are three principal vein orientations. East-north-east-trending veins are the most abundant and yielded a substantial proportion of the orefield's major lead oreshoots. A set of mainly north-north-west-trending veins are generally barren or only poorly mineralised, though they are associated with economic mineralisation in parts of the Alston and Nenthead areas. A third set of roughly east–west-trending fractures, though fewer in number, include some of the longest known veins in the orefield. Unlike the other orientations, these typically occupy sinistral transcurrent faults and commonly carry substantial widths of fluorite and/or quartz, but are generally poor in sulphide minerals. Stratabound mineralisation is associated with veins of all three principal directions.

In terms of wall-rock lithology, hard, competent wall-rocks, such as limestone or sandstone, generally provide steeply inclined, clean, open fissures favourable for deposition of wide vein oreshoots. In weak, incompetent rocks, such as mudstone, fissures are usually more gently inclined and were normally closed, preventing their filling by mineralising fluids. Vein fillings commonly exhibit a banded texture with pure, or almost pure, continuous to discontinuous bands of constituent minerals generally parallel to the vein walls. Ore minerals commonly form discontinuous bands, often, though not invariably, occupying a central position in the vein. Open vugs lined with euhedral crystals of the constituent minerals are common, frequently in the centres of veins. Many veins show numerous repetitions of mineral bands and no general paragenetic sequence of filling can be established.

A marked zonation, particularly of gangue minerals, is a characteristic feature of the North Pennine Orefield in the Alston Block, and may be envisaged as dome-shaped zones that exhibit a clear relationship to the form of underlying Weardale granitic batholith. Within a central zone both veins and stratabound orebodies are typically dominated by abundant fluorite (Figure 1). Local centres of copper-rich mineralisation, in places accompanied by some bismuth, rare earth element minerals and rare traces of cassiterite, have also been identified in early quartz–sulphide portions of veins in this central zone (Ixer, 1986; Ixer et al., 1996; Ixer and Flowers, personal communication *in* Dunham, 1990). Within the central zone fluorite-bearing veins locally pass downwards into deeper zones dominated by quartz and iron sulphides. Numerous studies of fluid inclusions

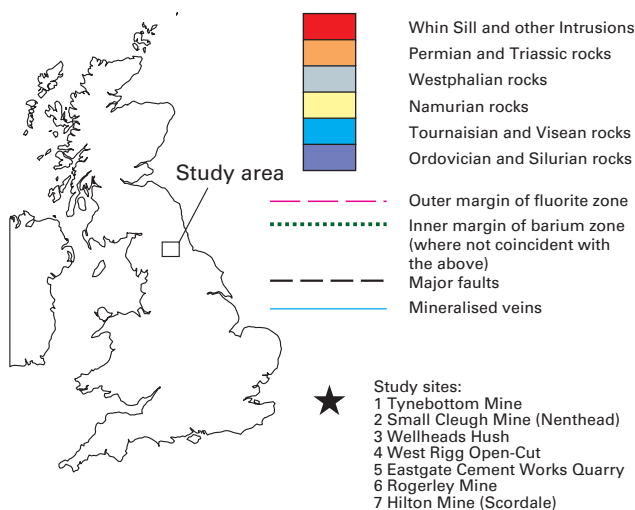
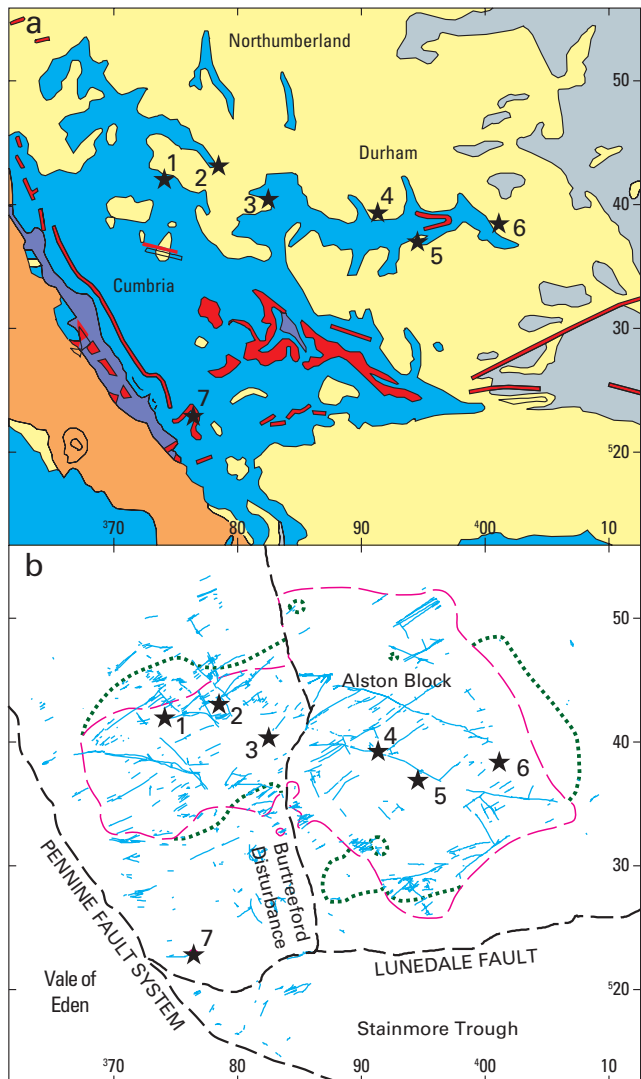


Figure 1 The location, structure and geology of the North Pennine Orefield.

a Generalised geology of the study area, along with the positions of the studied deposits.

b Main structural elements and the positions of the mineralised veins in the area.

in quartz and fluorite from the fluorite zone indicate homogenisation temperatures of up to 210°C (Dunham,

1990), with cooler temperatures (below 130°C) recorded towards the margins of the fluorite zone (Sawkins, 1966). The fluids were predominantly high salinity NaCl–CaCl₂-brines (typically about 20% wt% NaCl equiv.) and enriched in K and Li relative to oilfield brines (Rankin and Graham, 1988; Cann and Banks, 2001). However, little published information exists on the relationship between cation ratios (e.g. Na to Ca) and the salinity of the fluids. Current models for mineralisation in the orefield typically invoke sulphide and fluorite precipitation in response to mixing of a metalliferous Cl-dominated brine (of various potential sources), with a sulphate-dominated brine (e.g. Solomon et al., 1971; Solomon et al., 1972; Dunham, 1990; Crowley et al., 1997; Cann and Banks, 2001).

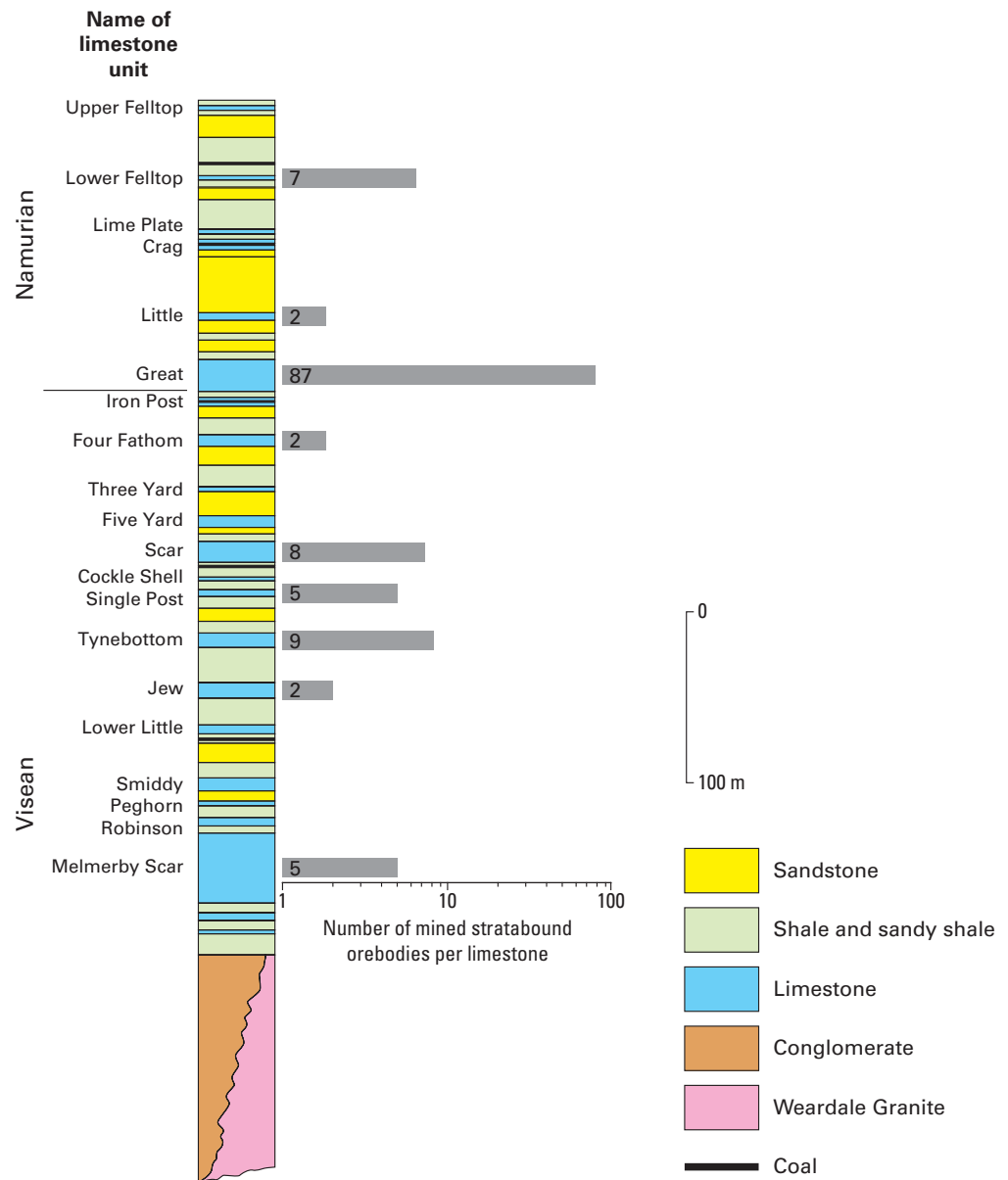
Surrounding the fluorite zone is a wider outer zone in which the gangue assemblage is dominated by barium minerals. The transition from the fluorite to the barium zone is generally very sharp—fluorite and barium minerals are normally mutually exclusive. Fluid inclusion homogenisation temperatures of between 100 and 125°C have been recorded from barite within the outer zone of the orefield, but Dunham (1990) has suggested that much of the barite may have been formed at temperatures below 70°C. Unlike the Pennine orefields of the Askrigg Block and Derbyshire, only in a few deposits in the Alston Block do fluorite and barium minerals occur together in the same deposit. Where this relationship is seen, fluorite is the earlier mineral. Barite is probably the most abundant barium mineral in the barium zone, though the Alston orefield is unique for the widespread abundance of the witherite [BaCO₃], together with much smaller quantities of barytocalcite and alstonite [BaCa(CO₃)₂ polymorphs].

The mineralisation is considered to have been initiated shortly after, or during, the cooling of the c.295 Ma Whin Sill (Fitch and Miller, 1967; Young et al., 1985; Dunham, 1990), and to have continued into the Permian. However, consideration of the available radiometric data (Dunham et al., 1968; Shepherd et al., 1982; Davison et al., 1992; Lenehan, 1997) suggests that the main phase of mineralisation was restricted to the period between the latest Permian (c.250–260 Ma) and the end of the Triassic (c.210 Ma; Cann and Banks, 2001).

1.2 STRATABOUND MINERALISATION IN THE NORTH PENNINE OREFIELD

In the North Pennine Orefield, stratabound mineralisation accounted for a substantial proportion of the commercial output of lead, zinc and iron ores, as well as significant tonnages of barite and witherite. The extensive stratabound mineralisation within the Great Limestone (Figure 2) at Boltsburn (Weardale) and Allenheads (East Allendale) mines (Figure 1) comprised two of Britain's largest and most productive lead orebodies. Approximately 250 000 tons of lead concentrates are recorded from the latter mine, a substantial proportion of which was obtained from stratabound deposits. Similar deposits, also within the Great Limestone, yielded large tonnages of both lead and zinc ores at several mines in the Nenthead area. Stratigraphically lower limestones have generally been little explored in the orefield although, where such exploration has occurred, significant mineralisation has been found, notably within the Tynebottom Limestone at Rotherhope Fell Mine, near Alston. The discovery of zinc-rich mineralisation in even lower limestones in the Rookhope Borehole (Dunham et al., 1965) and in the deepest workings of Cambokeels Mine, Weardale, may point to significant potential for economic

Figure 2 Generalised stratigraphy of the North Pennine Orefield, showing the stratigraphic location and distribution of the main stratabound orebodies. Log-scale axis represents the number of mined stratabound orebodies per limestone. Major concentration of orebodies were located in the Great Limestone, but they were also found in limestones above (up to 150 m) and below (up to 400 m) this horizon (modified after Sawkins, 1966; oreshoot data from Dunham, 1990).



stratabound mineralisation at depth. Important stratabound deposits of barite were mined at Silverband, Dufton, Murton and Hilton mines on the Pennine escarpment and large stratabound deposits at Nentsberry Mine, Nenthead are known to contain substantial tonnages of mixed sphalerite and witherite ore. Also, large stratabound deposits, mainly in Weardale, mainly in the form of oxidised or partially oxidised siderite and ankerite, provided significant quantities of iron ore.

Despite former economic importance, the stratabound mineralisation has attracted little research interest compared to the numerous veins with which they are associated. Numerous good surface and accessible underground exposures of this style of mineralisation remain throughout the orefield and these form the basis for this report (Figure 1). Included here are some of the better-known and most productive examples of their type. However, most of the largest and most productive regions of stratabound mineralisation are now inaccessible and, although numerous specimens of individual minerals are preserved in museum collections, only limited amounts of material and scientific observations remain suitable for genetic studies.

Dunham (1948; 1990) provided the most detailed and comprehensive observations of these deposits, including

some contemporary descriptions, and it is appropriate here to summarise some of the most pertinent. The stratigraphical distribution of worked stratabound mineralisation, based largely upon Dunham's work, is summarised in Figure 2.

Stratabound mineralisation is found only in association with veins accompanied by numerous diverging strings, sub-parallel 'leaders', or in the vicinity of vein intersections. In addition it appears to be developed in association with strong veins where, due to a variety of stratigraphical or structural constraints, vein oreshoots were not formed. Contemporary records of mines such as Allenheads and Boltsburn reveal several instances of extensive stratabound mineralisation in the Great Limestone where it is overlain by impervious mudstone, but vein oreshoots were normal in situations where sandstones directly overlie the limestone. This implies a strong hydrological and lithological control to the mineralisation. In addition the stratabound deposits at Rotherhope Fell Mine, near Alston and St Peter's Mine, East Allendale, hosted in the Tynebottom and Great limestones respectively, both occur within the crests of gentle anticlines.

Mine plans (Dunham, 1990) give an excellent view of the scale and morphology of the mineralisation. In general they are elongated in the direction of the associated vein and,

where mined, they are typically between 5 and 20 m wide and up to 3 m thick. They can also be lobate in plan, locally with pillar structures of apparently unmineralised ground. Though the mineralisation is classed as metasomatic in origin (Dunham, 1990), field observations (Figure 3) and historical mining accounts, suggest significant open-space mineralisation on a local scale. At Small Cleugh mine (Site 2), the mineralised zone contained metre-sized cavities lined with ankerite and/or quartz together with galena and sphalerite (Sopwith, 1833).

1.3 MATERIALS AND METHODS

Mineralised samples were collected from stratabound mineralisation at seven sites (Figure 1), including the formerly economically important Small Cleugh and Hilton flats. However, access to other major stratabound deposits, such as Boltsburn and Allenheads flats, is no longer possible. Although we can make use of contemporary records for comparison purposes, our observations may not be wholly representative of the mineralisation style.

Petrographic, fluid inclusion and mineral microchemical analyses were conducted on polished thin-sections and doubly polished, free-standing fluid inclusion wafers using a variety of techniques. Cathodoluminescence (CL) observations were made using Technosyn Mark II apparatus. Backscattered electron scanning electron microscope (BSEM) analyses were conducted using a LEO 435VP microscope with Oxford Instruments ISIS300 energy dispersive X-ray analyser (EDXA). Microchemical mapping and point analyses of carbonates were undertaken using a Cameca SX-50 electron microprobe (EPMA). Fluid inclusion microthermometric data for fluorite, quartz, dolomite/ankerite and calcite were collected using a computer controlled Linkam MDS600 heating–freezing system calibrated against synthetic fluid inclusions. The general methodology used was that outlined by Goldstein (2001) and references therein. For monophase inclusions, salinity was determined by cryogenically or thermally stretching the inclusion to induce the nucleation of a vapour phase. The errors in determining homogenisation temperature (T_h), first melting (T_{fm}), last ice-melting (T_{ice}) and hydrate melting (T_{hyd}) are typically $\pm 5^\circ$, $\pm 0.2^\circ$, $\pm 5^\circ\text{C}$ and $\pm 0.2^\circ\text{C}$ respectively. Where paired T_{ice} and T_{hyd} were available, CalcicBrine (Naden, 1996) was used to calculate salinities in terms of the system $\text{NaCl}-\text{CaCl}_2-\text{H}_2\text{O}$. In the absence of T_{hyd} data, salinities were calculated in terms of the system $\text{NaCl}_2-\text{H}_2\text{O}$ for $T_{ice} \geq -21.3^\circ\text{C}$ and in the system $\text{CaCl}_2-\text{H}_2\text{O}$ for $T_{ice} < -21.3^\circ\text{C}$. No pressure corrections have been applied to the homogenisation temperatures. The majority of inclusions analysed were of primary ($n=241$) origin, with fewer pseudosecondary ($n=45$) and secondary ($n=47$) inclusions. Comparison of data from the different

fluid inclusion generations reveals no detectable differences in character between the different types. The samples were also screened using epifluorescence which failed to reveal any hydrocarbon-bearing inclusions.

Fluid inclusions were ablated with a Geolas Q Plus excimer laser (ArF, 193 nm) and the ablated material analysed using an Agilent 7500c quadrupole ICP-MS fitted with a dynamic reaction cell. The optical delivery system was that described by Gunther et al. (1997a). The sample ablation cell has a volume of approximately 13 cm^3 and the ablated material was removed from the cell in a stream of He gas (0.68 l/min) and premixed with Ar (0.95 l/min) before introduction to the plasma. Calibration was carried out using a combination of NIST reference glasses SRM 610 and 612 and aqueous standards ablated directly through the walls of glass capillaries (Gunther et al., 1997b; Allan et al., 2006). Analytical precision for Li, Na and K is typically better than 15% relative standard deviation (RSD), while Mg, Cl, Ca, Mn, Fe, Cu, Zn, Sr, Ba and Pb are reproducible within 30% RSD. Accuracy for most elements is within 15% (Allan et al., 2006). Isotope masses (^7Li , ^{23}Na , ^{24}Mg , ^{35}Cl , ^{39}K , ^{44}Ca , ^{55}Mn , ^{57}Fe , ^{63}Cu , ^{66}Zn , ^{88}Sr , ^{137}Ba , ^{208}Pb) were selected so as to minimise potential interferences. Although ^{57}Fe is relatively interference-free, some of the analyses were carried out under conditions where the reaction cell was pressurised with 2.5 l/min H_2 to eliminate interference from the $^{40}\text{Ar}^{16}\text{O}^+$ dimer on the $^{56}\text{Fe}^+$ and greatly reduces high Ar-based backgrounds on $^{39}\text{K}^+$. The use of a hydrogen reaction cell also precluded the analysis of Li and Cl. Limits of detection (i.e. $3 \times \text{sigma}$ on background counts) vary according to inclusion mass (volume \times concentration of analyte) but are generally 1 to $102\mu\text{g/g}$ for most elements. For data interpretation, Na was used as the internal standard; the concentration of Na being estimated from independent microthermometric calculations. Data processing was undertaken using in-house software ('SILLS' written by Murray Allan, Dept. Earth Sciences, University of Leeds).

Samples of host limestones, dolostones and open-space-filling dolomite, ankerite and calcite were extracted using micro-drills and analysed for $\delta 18\text{O}$ and $\delta 13\text{C}$ using a procedure based on the methodology of McCrea (1950). The various carbonate minerals were reacted at different temperatures according to their thermal stability — calcites were reacted at 25.2°C (Friedman and O'Neil, 1977), dolomites and ankerites at 100°C (Rosenbaum and Sheppard, 1986). Analyses were undertaken on a VG Optima dual-inlet gas-source mass spectrometer. Each batch of unknown samples was run with three primary standards with known values with respect to NBS-19. The resultant gas values were further adjusted using Craig's correction for small levels of ^{17}O isotopes. The values were normalised through the primary standard and corrected to the solid carbonate value using a fractionation factor to account for the incomplete liberation of the oxygen in phosphoric acid.

2 Results

2.1 SITE DESCRIPTIONS

Tynebottom Mine (Site 1 — Figure 1; grid reference 3739 5418)

This is a comparatively small lead mine developed at the intersection of the east-north-east-trending Dryburn Washpool–Browngill Vein, one of the main feeder channels of mineralisation in this part of the orefield, with a roughly north-west-trending vein known as Windshaw Bridge Vein. Lead oreshoots occurred here both in vein and stratabound orebodies hosted in the Dinantian Tynebottom Limestone. The stratabound mineralisation extended for at least 244 m along both the Dryburn Washpool–Browngill and the Windshaw Bridge Veins (Dunham, 1990). It averaged about 6 m in width but increased to as much as 15 m wide near vein intersections. Underground workings show good representative sections through unworked portions of both the stratabound mineralisation and the veins. The host limestone is replaced by fine-grained quartz and chalcedony, forming a very hard dark grey siliceous rock, through which are disseminated crystals of galena, marcasite and pyrite. Numerous vugs in this altered rock are lined with quartz, calcite, ankerite and, in places, purple fluorite (Dunham, 1990). Other minerals present include pyrite, arsenical marcasite, galena and sphalerite, with minor amounts of glaucodot, gersdorffite, chalcopyrite, pyrrotite, ullmanite (Ixer, 1986; Vaughan and Ixer, 1980) and traces of the rare earth mineral synchysite (Ixer and Stanley, 1987).

Small Cleugh Mine (Site 2 — Figure 1; grid reference 3787 5430)

This is one of a number of workings within the upper part of the Nent Valley that produced galena and sphalerite from an extensive zone of stratabound mineralisation. These are associated with a series of north-north-west-trending cross veins in the Namurian Great Limestone. Normally in the North Pennine Orefield, veins with this trend are barren or only weakly mineralised, but at Nenthead they are locally well mineralised and commonly associated with extensive stratabound mineralisation in the adjoining limestone. The stratabound mineralisation occurs within a horst structure, up to 213 m wide, between two cross veins. It extends over a total strike length of over 1.1 km and a volume of at least $3.5 \times 10^6 \text{ m}^3$ (Dunham, 1990).

Underground extraction has created a large network of caverns, the extent of which gives a clear indication of the limits of economic mineralisation. However, large areas of stratabound mineralisation remain exposed in the walls of the workings indicating that the full extent of the replacement mineralisation is greater than revealed by the present excavations. These exposures show the Great Limestone to be extensively replaced, mainly by ankerite, siderite and some fine-grained silica, giving an intensely hard, generally medium to dark grey crystalline rock. In the most intensely mineralised beds, zebra dolomites and vugs, typically lined with curved rhombic crystals of cream coloured ankerite in places accompanied by quartz, calcite and ore minerals, are extremely common. Galena and sphalerite occur as coarsely crystalline lenses and

bands within the altered limestone and are common as well crystallised masses within vugs.

Wellheads Hush (Site 3 — Figure 1; grid reference 3825 5403)

This is an ancient opencast working near the head of Weardale where lead ore was worked from three converging roughly east-north-east-trending veins and associated replacement deposits in the Great Limestone. Although the individual veins are no longer clearly exposed, they appear to be no more than 1 m wide. However, over a strike length of about 100 m the Great Limestone exhibits strong stratabound mineralisation with ankerite, siderite and minor fluorite and galena over widths of up to 15 m.

West Rigg Open cut (Site 4 — Figure 1; grid reference 3911 5392)

This is a large abandoned quarry which worked a replacement deposit of 'limonitic' ironstone associated with the Slitt Vein, the longest vein in the orefield, within the Namurian Great Limestone. The vein strikes roughly east–west and at West Rigg is up to 5 m wide over a strike length of around 200 m. Like other east–west-trending veins it carries large amounts of quartz and some fluorite, but has uneconomic concentrations of galena. Adjacent to the vein, almost the full 18 m thickness of the Great Limestone has been replaced by limonitic ironstone, derived from the supergene alteration of primary carbonates, almost certainly siderite and ankerite. Iron mineralisation here locally extends for up to 61 m on either side of the vein. Although almost totally extracted, small exposures of iron ore remain locally in the walls of the workings. Slitt Vein itself remains as an unworked rib, which forms a prominent wall-like feature across the centre of the quarry (Figure 3a).

Eastgate Cement Works (Site 5 — Figure 1; grid reference 3947 5368)

Limestone and shale was extracted from the Great Limestone and overlying beds in this quarry. In places these beds are cut by several small, mainly roughly east–west-trending, mineralised faults that appear to be branches from Slitt Vein, which crops out to the north of the quarry. These veins appear to be less than 1 m wide but are locally associated with significant stratabound mineralisation extending for several metres on either side of the vein. Ankerite, siderite and quartz dominate the stratabound assemblage but are accompanied by abundant purple and green fluorite, galena, quartz and aragonite in numerous vugs.

Rogerley Mine (Site 6 — Figure 1; grid reference 4009 5384)

This is a very small mine within Rogerley Quarry, Frosterley, near the eastern end of Weardale. The mine is developed in the roughly north-east-trending vein that cuts the Great Limestone. It consists mainly of fluorite and galena and is generally less than 1 m wide, but the adjacent limestone

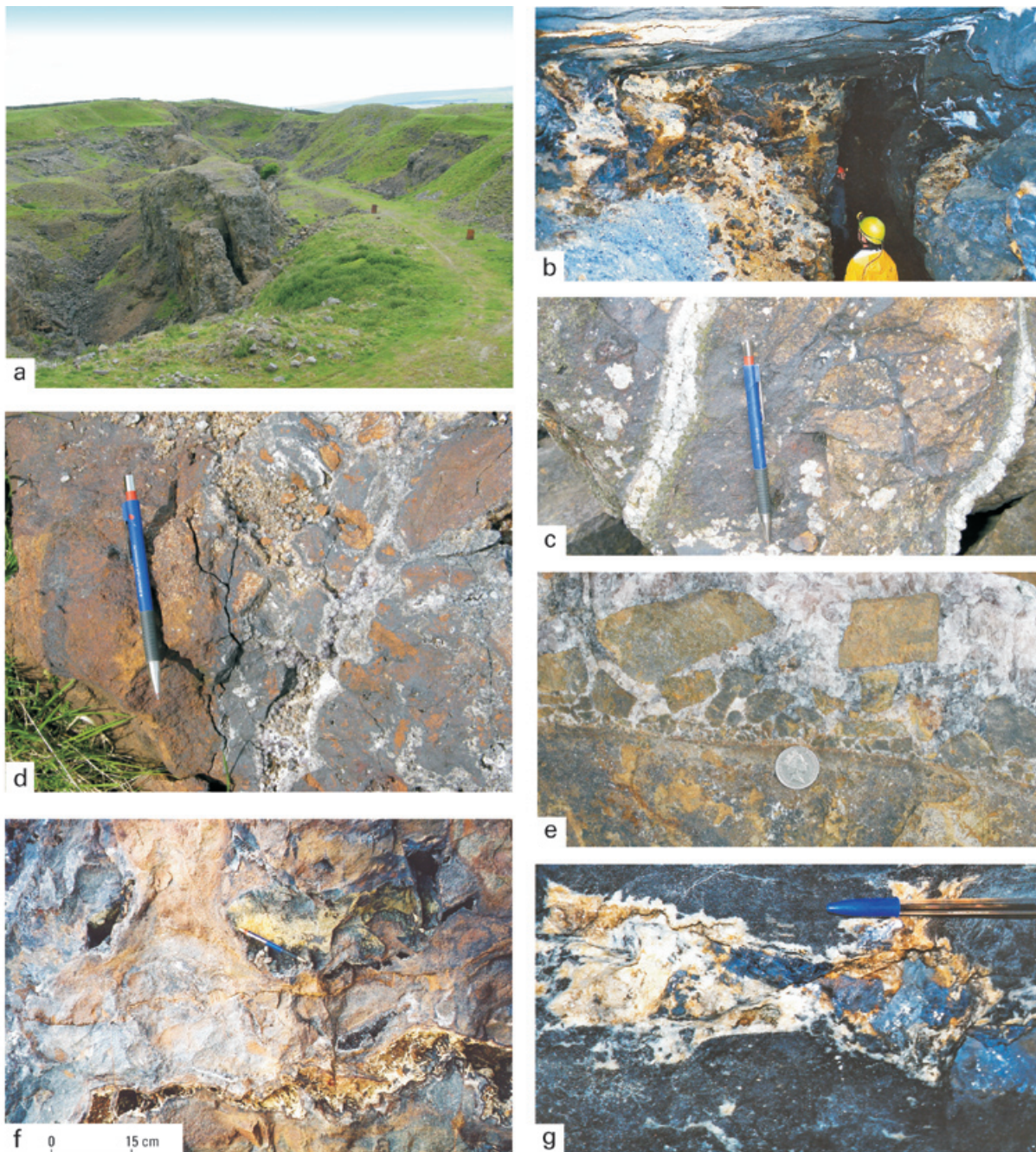


Figure 3 Mineralisation styles associated with stratabound mineralisation in the North Pennine Orefield.

a View of West Rigg disused iron works, showing the general size and form of the stratabound mineralisation.

b Flat-vein-style mineralisation. The geologist is standing within the mined-out cavern of the main vein. The main vein narrows into a very thin fissure where it meets a thin clay layer at the bottom of the overlying, unmineralised limestone, but directly below this the mineralisation is seen to extend as a series of sub-horizontal veins that may include rafts of host rock, into the adjacent limestone (Tynebottom Mine).

c Minor mineralised veining and stockwork of intersecting fractures with adjacent Fe-metasomatism of dolostone (West Rigg Open-cut).

d Stockwork of fluorite veins in altered dolostone, with intersecting, dissolution-enhanced, veins/fractures leading to generation of jig-saw fit breccia. Also developed are dm-scale vuggy pores lined with fluorite (Wellheads Hush).

e Fluorite-cemented breccia with size-graded angular clasts of dolostone resting upon a mineralised dolostone surface (Eastgate Cement Works Quarry).

f Network of large vuggy pores with a preferred orientation sub-parallel to bedding. These vugs developed after some veining as is shown by the preserved vug-spanning fracture in the bottom left corner of the image. The vugs are lined by fluorite and carbonate with a late encrustation of smithsonite/cerussite (Eastgate Cement Works Quarry).

g Sub-horizontal vuggy porosity within dolostone. The vug margins are irregular at the mm to cm scale and are lined by creamy-white ankerite. Coarsely crystalline galena is developed in the centre of the vug (Small Cleugh Mine).

is extensively replaced by mainly fine-grained silica and ankerite in which occur numerous large, irregular vugs, typically up to 1 m or more across and up to 1 m high, lined with clear, euhedral, interpenetrating cubes of deep green fluorite up to 3 cm across. Many of these vugs are filled, or partially filled, with stiff greyish brown clay. Whereas this may represent insoluble residues from limestone dissolution during mineralisation, it seems more likely that the clay was washed into the cavities from the surface during recent or Quaternary times. Rogerley Mine was developed solely to produce fine specimens of well-crystallised green fluorite.

Hilton Mine (Site 7 — Figure 1; grid reference 3764 5228)

This is one of a number of abandoned surface and underground workings that worked lead ore, barite and some witherite from a number of mainly east-north-east-trending veins and associated stratabound deposits within Carboniferous limestones. The Carboniferous rocks are here intruded by a Permo–Carboniferous dolerite intrusion known as the Whin Sill, which at Hilton Mine is emplaced immediately above the roughly 100 m thick Melmerby Scar Limestone (Figure 2), and overlying shale. The intrusion has metamorphosed the adjoining limestone to marble and the shale to a fine-grained hornfels. Although several vein orebodies have been worked here, mineralisation occurs mainly as a series of extensive stratabound deposits associated with veins within the altered Melmerby Scar Limestone and overlying shale. Individual orebodies were up to 300 m long, 37 m wide and up to 1.8 m thick (Dunham, 1990). Examination of the remaining accessible portions of these deposits reveals that substantial portions of the altered limestone have been replaced by granular crystalline fluorite, together with abundant barite and some galena. However, much of the stratabound mineralisation accessible today appears to be concentrated within the thin (approximately 1 m) hornfelsed shale which overlies the Melmerby Scar Limestone and which is in turn overlain by the lower contact of the Whin Sill. Within these parts of the mineralisation, hornfelsed shale breccia clasts are commonly cemented by coarsely-crystalline yellow fluorite, white barite and smaller quantities of coarsely crystalline galena. Fluorite typically occurs as euhedral interpenetrant cubes up to 3 cm across, commonly overgrown or enclosed by radiating aggregates of tabular barite crystals up to 10 cm long.

2.2 STYLES OF STRATABOUND MINERALISATION

Throughout the orefield, metasomatism is mainly expressed as ankeritisation and sideritisation of the host limestones with replacement of pre-existing textures, including exceptional replacement of fossils by galena. Localised replacement of limestone by fluorite, quartz, barite, witherite and baritocalcite is also present. However, in addition to metasomatism, the following styles of stratigraphically confined mineralisation were also observed:

FLAT-STYLE VEINING (Figure 3b). This style is particularly distinctive and occurs where main veins are truncated by overlying impermeable soft beds and unmineralised limestones. Immediately below the truncation surface, the mineralisation extends laterally as a series of fractures subparallel to bedding, which may contain rafts of host rock. These characteristics are consistent with confinement of the mineralising fluids, with concomitant dissolution,

fracturing and mineralisation immediately below the impermeable barrier. Good examples of this style occur at Tynebottom Mine.

STOCKWORK-STYLE VEINING (Figure 3c). The smallest fractures and veins occur at the mm- to cm-scale and are characterised by Fe-Mn metasomatism in the adjacent host rocks and by fluorite cementation. These locally form interlocking stockworks which grade into jigsaw-fit breccias.

MINERALISED BRECCIAS (Figures 3d and e). Two types of mineralised breccia are observed: (i) jigsaw-fit breccia with pervasive cementation by carbonate ± fluorite ± quartz, commonly accompanied by alteration at clast margins. (ii) Angular clasts of ankeritised limestone resting upon ankeritised host limestone, with sharp basal contacts and reverse grading. In the latter type, clasts are irregularly aligned with respect to their primary bedding planes, display poor degrees of fit, and are typically cemented by later minerals including fluorite and quartz. This type is interpreted to represent the collapse of material from the margins of developing fracture or vuggy porosity.

MINERALISED VUGS (Figures 3f and g). Sub-horizontal lenticular cavities in ankeritised limestone commonly have irregular margins and are typically lined with a range of ore and gangue minerals with well-developed, commonly very coarsely crystalline (cm-scale) euhedral morphologies, indicating growth into open space. Earlier fractures commonly cut across vugs, and are preserved intact where the adjacent host rock has been dissolved, indicating that at least some veining predates vug formations (Figure 3f). However, some fractures and veins terminate at the margins of vugs indicating that fracturing post-dates porosity generation. The presence of the same mineral assemblage within the veins as within the vugs, suggests that in these cases, the veins have acted as feeders bringing mineralising fluids into the open vug space. A good example of this style of mineralisation is found in the Jew Limestone at Cambokeels Mine, where horizontal rafts of limestone lie in a mainly quartz–fluorite matrix. This is illustrated by Dunham (1990; Plate 7).

2.3 PETROGRAPHY, FLUID INCLUSION MICROTHERMOMETRY AND MINERAL CHEMISTRY

The minerals associated with diagenetic overprinting and mineralisation of the limestones are described below, in approximate paragenetic order, along with a description of their known fluid-inclusion and stable-isotope characteristics. However, the main ore and associated gangue minerals show highly variable paragenetic relationships, in some cases with repeated cycles of fluorite–sulphide-dominated and quartz-dominated mineralisation, commonly associated with brecciation and re-cementation of earlier mineral fills.

2.3.1 Limestone texture and diagenesis

The limestones that host the mineralisation are bioclastic grainstones and wackestones with abundant, variably luminescent, crinoid, brachiopod and other bioclasts (e.g. Dunham, 1990). The grainstones are typically pervasively cemented by non-luminescent, sparry-calcite cement, whereas the micrite matrices of the wackestones tend to be dully luminescent. No early marine cements such as acicular or isopachous aragonite or high-Mg calcite have been observed, indicating probable overprinting by

subsequent diagenetic and mineralisation episodes. EPMA indicates that both the detrital bioclasts and the cements have similar compositions with very low Mn and Fe contents (typically <0.01 formula units Fe and Mn, when analyses are normalised to 2 cations; Figure 4). Mg contents are marginally higher (typically in the range 0.01–0.06 formula units). Sr is also present in low concentrations (< 0.01 formula units). These Sr concentrations are notably higher than those observed in the later calcite veining and carbonate alteration products described below, and possibly represent a geochemical signature inherited from precursor marine cements (Tucker and Wright, 1990).

Fluid inclusions within these cements have relatively low salinities (typically <6 wt% saltequiv.; Figure 5a and Figure 6), and T_{fm} (c. –25°C) indicative of a NaCl-bearing fluid. Homogenisation temperatures are highly variable (75–160°C; Figure 5c), and this is probably indicative of inclusion leakage during subsequent diagenesis and mineralisation. Limited stable isotope data (n=4) from unaltered limestones indicates variable $\delta^{18}\text{O}_{\text{PDB}}$ of –12.2 to –5.7‰, and $\delta^{13}\text{C}_{\text{PDB}}$ between –5.7+1.5‰ (Table 1 and Figure 7).

2.3.2 Anhydrite and gypsum

Within some of the more muddy limestones and dolostones, lath-shaped pores lined or filled by later generations of minerals (predominantly quartz) suggest that gypsum and/or anhydrite formerly occurred, though none remain today.

2.3.3 Dolomite

Dunham (1990) noted that most of the minerals previously classified as dolomites were in fact ankerites. However, here we document the presence of dolomite *sensu stricto*. In the vicinity of the veins and stratabound mineralisation, the limestone is typically pervasively dolomitised or ankeritised with the development of idiotopic-subhedral (using the classification of Gregg and Sibley, 1984), mosaics of interlocking, predominantly non-luminescent dolomite crystals, with varying amounts of interstitial fines, probably reflecting the clay content of the precursor limestone. Dolomitisation locally preserves relics of primary fabrics and bioclasts are sometimes preserved in dolomite crystal cores, suggesting nucleation upon, but incomplete replacement of, these clasts (Figure 8a). Dolostones are locally stylolitised indicating that compaction continued after dolomitisation. Dolomite in the host rocks has variable Fe and Mn contents. At Wellheads Hush, the dolomite is Fe and Mn rich, but Sr poor (>0.5, > 0.04 and <0.001 formula units respectively; Figures 4d, e and f). At Small Cleugh Mine, Fe and Mn contents are variable (0.1–0.3 and 0.01–0.12 formula units respectively), but Sr contents are low (typically less than 0.001 formula units). At Rogerley Mine, Fe and Mn-contents are low (less than 0.1 and less than 0.01 formula units respectively) whereas Sr contents are high (between 0.003 and 0.01 formula units; Figure 4c and d).

Due to the cloudy nature of the dolomite and the very small sizes of fluid inclusions, it only proved possible to acquire limited freezing run data from the dolomite host rocks. However, these indicate high salinities (18–23 wt%, mean 21 wt% salt equiv), and suppressed T_{fm} (–55 to –35°C) consistent with the presence of cations additional to Na and Cl within the fluid. Unfortunately no T_{hyd} data could be collected, which prevented modelling of the relative proportions of NaCl and CaCl₂. Homogenisation temperatures are within the relatively narrow range of 110–130 °C. The small size of the inclusions precluded the acquisition of fluid inclusion microchemical data.

The dolomitised host rocks have variable $\delta^{18}\text{O}_{\text{PDB}}$ and $\delta^{13}\text{C}_{\text{PDB}}$ ratios (–12.9 to –5.6‰ and –7.3 to +1.3‰ respectively) with no coherent co-variations observed between the two isotope systems (Figure 7). Using the fractionation factors of Friedman and O'Neil (1977), the d18OSMOW of fluid in equilibrium with dolomite of this composition at the temperatures suggested by the fluid inclusion homogenisation data (120°C) is in the range –2.2 to +5.4‰.

2.3.4 Ankerite

This is typically the earliest porosity-filling phase in the fractures and vugs of the stratabound deposits. It is typically coarsely crystalline (up to 5 mm in maximum dimension), with saddle-shaped projections (xenotopic-cement) into the centres of open pore space (Figure 8b). Fracture- and vug-lining ankerite compositions overlap with those described above for dolomite in the host rocks, with the earliest ankerite generations typically having compositions comparable to the dolomite host rock (Figure 4 and Figure 9). Later generations become progressively more ferroan and manganoan, although some oscillatory zoning with respect to these components is also evident. Sr contents are typically low (less than 0.001 formula units), although concentrations at Rogerley Mine are higher.

Rare zebra dolomites are also observed. These comprise alternating bands of black and white dolomite and ankerite stacked in an ABBABBA sequence (Nielsen et al., 1998; Wallace et al., 1994; Boni et al., 2000; Arne and Kissin, 1989). In common with other occurrences of zebra dolomite, the black dolomite occurs in thin (mm- to cm-scale), subparallel, sheet-like structures which comprise partially interlocking mosaics of idiotopic-subhedral, inclusion-rich, dolomite, commonly in a clayey matrix. The contact between the black and white dolomite is less clear in thin section than hand specimen observations would suggest, with progressively clearer dolomite forming syntaxial overgrowths on the matrix dolomite. As described above, the earlier generations are idiotopic-euhedral, but later generations become increasingly ferroan (ultimately to highly ankeritic compositions — Figure 9), with a corresponding increase in curvature of cleavage planes (xenotopic cement). For the two samples where paired isotope data are available for the black dolomite and white ankerite bands, the white ankerite is isotopically lighter in terms of both $\delta^{18}\text{O}$ and $\delta^{13}\text{C}$, with compositions comparable to that described below for vug- and vein-filling ankerite (Table 1).

Fluid inclusions in vein- and vug-lining ankerite have salinities (20–23 wt% salt equiv.) and eutectic melting temperatures similar to those in host rock dolomite, indicating a significant degree of similarity between the fluids responsible for dolomitisation and those responsible for the ankerite precipitation. However, homogenisation temperatures are more variable, with a broad distribution that spans the range 80–160°C. There is also a small population of monophasic inclusions within the ankerite, which we interpret to represent 'stretched' fluids, from the lower end of the observed homogenisation temperature frequency distribution (see discussion in Roedder, 1985).

Fracture- and vug-lining ankerite is characterised by typically lighter d18OPDB and $\delta^{13}\text{C}_{\text{PDB}}$ compositions than the dolomite within the host rocks (–14.9 to –10.7‰ and –5.2 to –1.4‰ respectively — Table 1), although there is some overlap between the outliers of each group when plotted together (Figure 7). The $\delta^{18}\text{O}_{\text{SMOW}}$ composition of water in equilibrium with this at 120°C, based on the fluid inclusion homogenisation data and using the fractionation factors of Friedman and O'Neil (1977) is in the range –4.2 to +0.1‰.

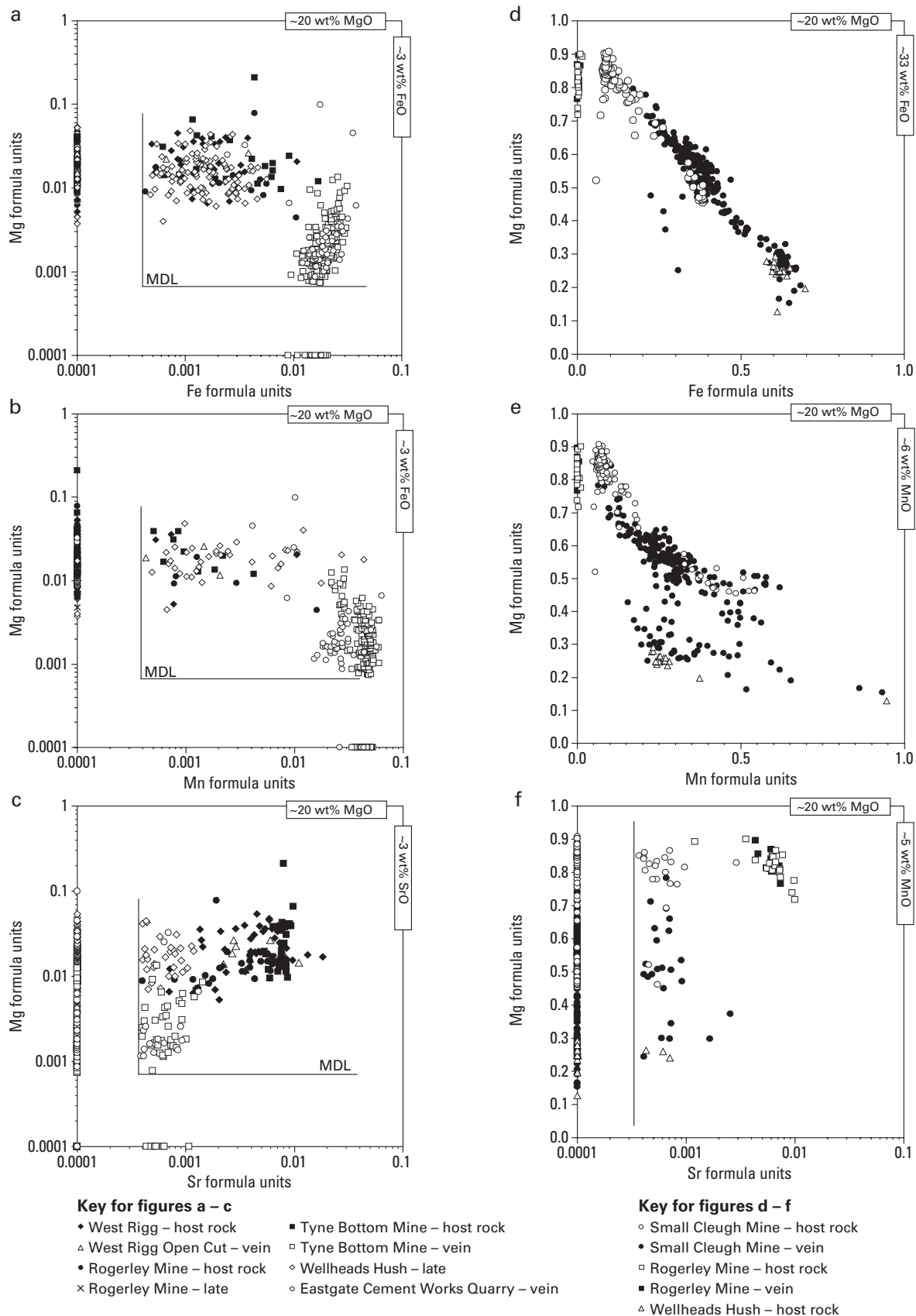


Figure 4 Summary plots showing co-variations in carbonate composition as determined by EPMA for calcite (a, b and c) and dolomite/ankerite (plots d, e and f). All data are plotted as formula units, with carbonate compositions calculated on the basis of two cations. Estimated minimum detection limits (MDLs) are indicated, and points falling below these limits are displaced to nominal concentrations of 0.0001 formula units on the appropriate axes. In d, e and f, host rock dolomite/ankerite is plotted using open symbols, and fracture/vug-lining dolomite is plotted using filled symbols. For all plots approximate oxide weight % equivalents are quoted on the X and Y axes, and a linear relationship between concentrations expressed as formula units and oxide weight % can be assumed for the purposes of approximation.

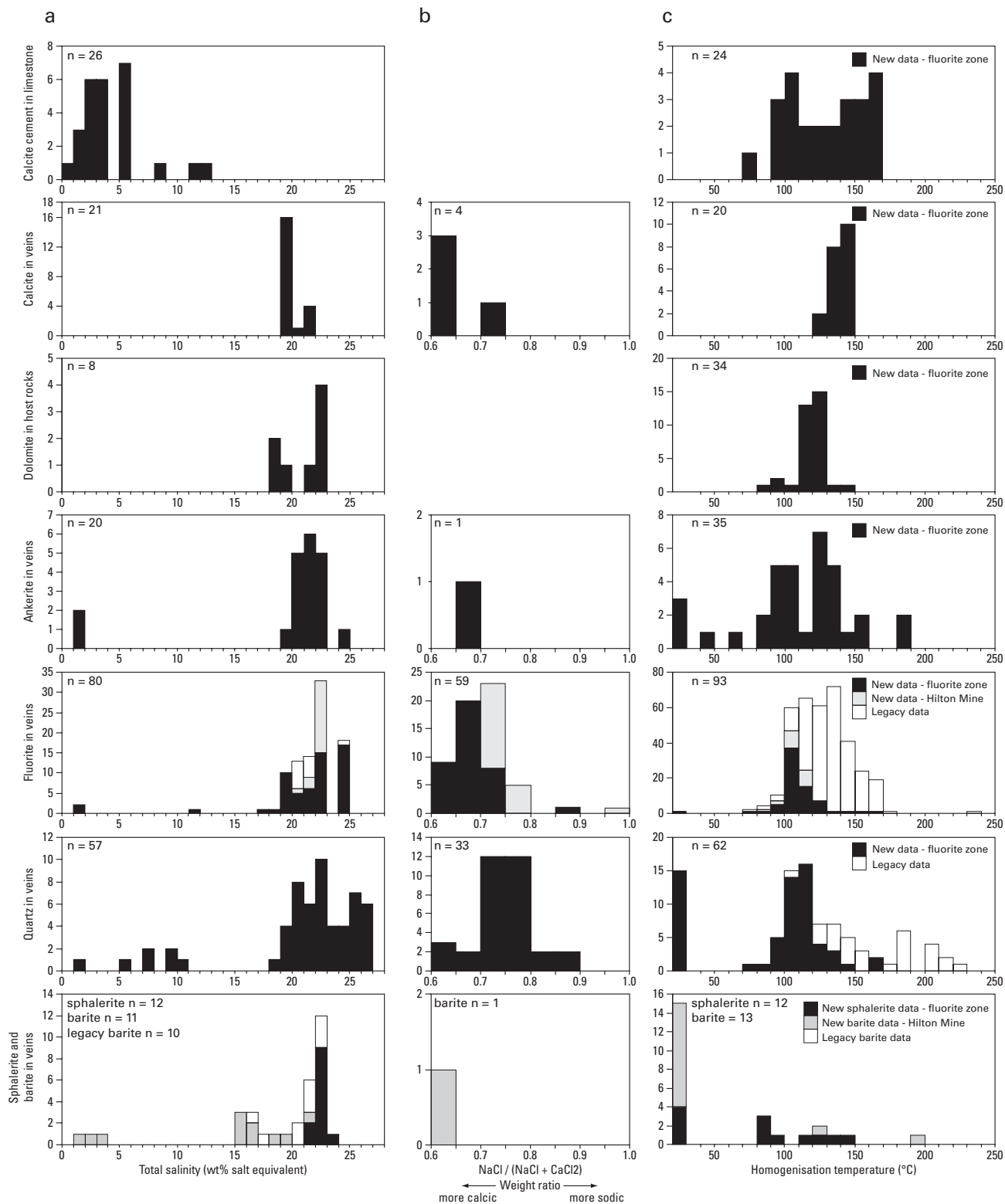


Figure 5 Histograms of fluid inclusion microthermometric data for samples of stratabound mineralisation in the North Pennines, with analyses plotted according to mineral and paragenetic position.

a Total salinity.

b Relative proportions of Na and Ca as modelled using CalcicBrine (Naden, 1996).

c Homogenisation temperatures, including proportions of monophasic inclusions for which no homogenisation data is appropriate. Legacy data from Smith (1974); Moore (1980); Christoula (1993) and Shepherd (unpublished).

Table 1 Stable isotope data for samples from the North Pennines. As the precise nature of the late carbonate encrustations is not known, $\delta^{18}\text{O}$ data for late carbonate encrustations are quoted using phosphoric acid fractionation factors for both smithsonite and cerussite (Gilg et al., 2003) — cerussite values in brackets.

Location	Mineral	Comment	Sample ID	$\delta^{18}\text{O}_{\text{PDB}}$ (‰)	$\delta^{13}\text{C}_{\text{PDB}}$ (‰)
1) Tyne Bottom Mine	Calcite	Limestone	NQ1033-01	-12.16	+1.51
		Vein calcite	NQ1033-02	-13.05	-3.42
2) Small Cleugh Mine	Dolomite	Grey dolostone	NQ1015-01	-9.92	-2.15
		Muddy dolostone	NQ1016-02	-7.27	+1.33
		Buff dolostone	NQ1016-03	-8.99	-0.44
		Grey dolostone	NQ1017-04	-8.12	+1.27
		Muddy dolostone	NQ1018-02	-7.84	+0.49
		Sphalerite-cemented dolostone	NQ1019-01	-9.58	-2.60
		Pale-grey dolostone	NQ1020-01	-10.84	-1.01
		Pale-grey dolostone	NQ1023-01	-7.30	+0.65
	Zebra Dolomite/ Ankerite	Black dolostone	NQ1017-01	-7.96	+0.57
		Vug-lining ankerite	NQ1017-02	-13.89	-2.61
	Ankerite	Muddy dolostone	NQ1022-01	-9.68	+0.71
		Vug-lining ankerite	NQ1022-02	-11.27	-5.18
		Vug-lining ankerite	NQ1015-02	-13.76	-3.87
		Vug-lining ankerite	NQ1015-03	-14.41	-3.28
		Vug-lining ankerite	NQ1016-01	-13.02	-4.62
		Vug-lining ankerite	NQ1018-01	-14.90	-3.19
	Pb/Zn Carbonate	Vug-lining ankerite	NQ1020-02	-11.19	-4.51
		Vug-lining ankerite	NQ1023-02	-10.74	-1.38
		Late carbonate encrustation	NQ1016-04	-9.16 (-9.16)	-6.91
		Late carbonate encrustation	NQ1016-04	-9.16 (-9.16)	-6.91
3) Wellheads Hush	Dolomite	Hematized dolostone	NQ1001-02	-7.04	-0.07
		Pale-grey dolostone	NQ1005-01	-9.72	+1.15
		Buff dolostone	NQ1005-02	-9.59	+1.05
		Hematized dolostone	NQ1006-02	-7.28	-0.93
		Pale-grey dolostone	NQ1007-01	-12.00	-7.28
		Hematized dolostone	NQ1008-02	-7.70	-1.95
	Pb/Zn Carbonate	Late carbonate encrustation	NQ1001-01	-5.64 (-5.18)	+0.87
		Late carbonate encrustation	NQ1002-01	-5.52 (-5.06)	-0.19
		Late carbonate encrustation	NQ1003-01	-5.69 (-5.22)	-0.27
		Late carbonate encrustation	NQ1006-01	-5.77 (-5.31)	+0.06
Late carbonate encrustation	Late carbonate encrustation	NQ1008-01	-5.62 (-5.16)	-4.66	
	Late carbonate encrustation	NQ1008-01	-5.62 (-5.16)	-4.66	
4) West Rigg Opencut	Calcite	Limestone	NQ1043-01	-11.97	+0.21
		Limestone	NQ1045-01	-5.69	-5.26
5) Eastgate Cement Works Quarry	Dolomite	Hematized dolostone	NQ1025-01	-11.79	-4.83
		Buff dolostone	NQ1026-01	-7.82	-0.60
		Pale-grey dolostone	NQ1027-01	-5.71	-1.77
		Buff dolostone	NQ1028-02	-6.72	-0.75
	Late Calcite	Late coarsely crystalline calcite	NQ1026-03	-11.74	-4.82
		Late coarsely crystalline calcite	NQ1028-01	-10.20	-4.24
	Pb/Zn Carbonate	Late carbonate encrustation	NQ1024-01	-5.83 (-5.37)	-1.39
		Late carbonate encrustation	NQ1026-02	-6.82 (-6.36)	-2.62
		Late carbonate encrustation	NQ1027-02	-6.76 (-6.30)	-1.61
		Late carbonate encrustation	NQ1046-01	-6.47 (-6.01)	-0.12
6) Rogerley Mine	Dolomite	Hematized dolostone	NQ1011-01	-7.59	-1.91
		Hematized dolostone	NQ1013-01	-12.99	+1.25
		Hematized dolostone	NQ1014-01	-8.08	-1.75
7) Hilton Mine	Calcite	Limestone	NQ1039-01	-7.67	-5.67
		Recrystallised limestone	NQ1041-01	-10.77	-3.34

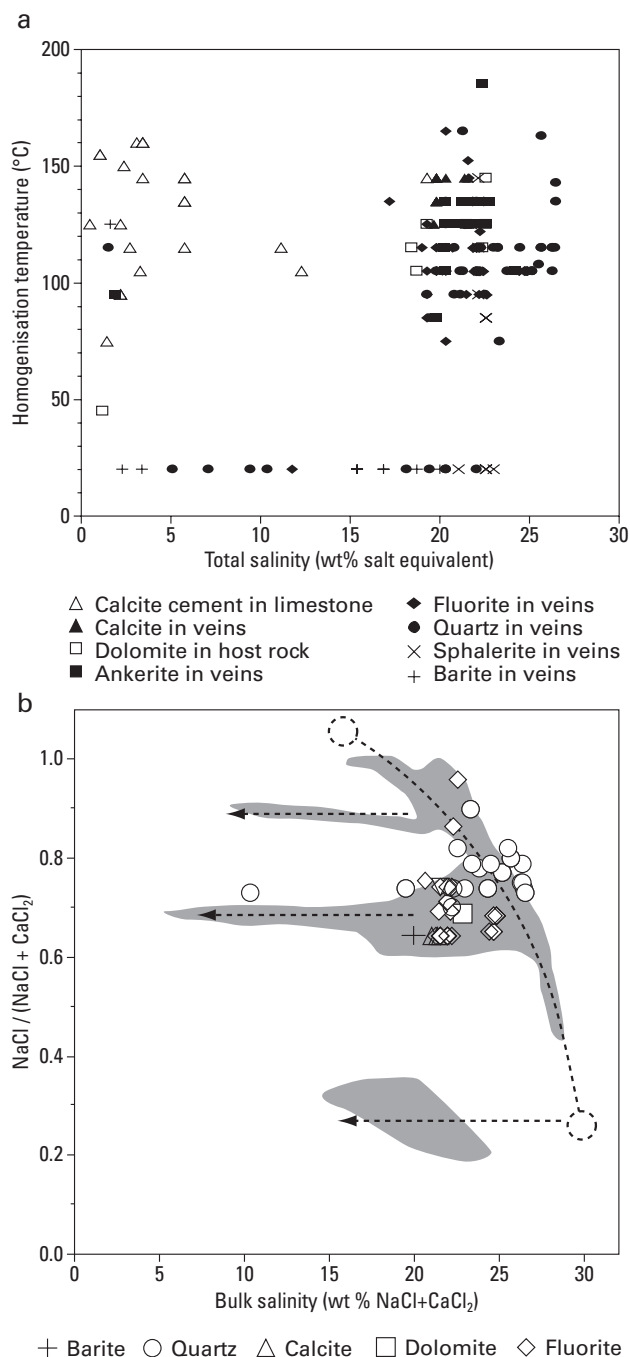


Figure 6 Cross plots showing variations in fluid inclusion salinity.

a Fluid inclusion salinity versus homogenisation temperature for samples of stratabound mineralisation in the North Pennines, with analyses plotted according to mineral and paragenetic position.

b Bulk salinity–NaCl/(NaCl+CaCl₂) plot. Shaded yellow fields show data for mixing between meteoric water and evolved sea and basinal brines from unconformity related Permo–Triassic mineralisation in Devon (Shepherd et al., 2005).

2.3.5 Fluorite

This forms fracture- and vug-lining, yellow, green, blue and purple coarsely-crystalline cubic euhedra of up to 2 cm diameter, which engulf the majority of the fracture/vug-lining ankerite described above. However, within certain fluorite

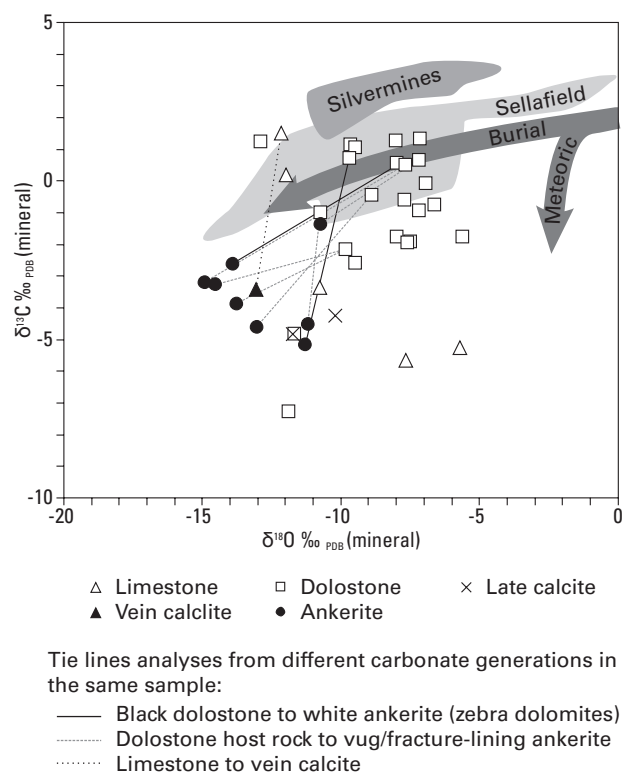


Figure 7 Stable isotope cross plot ($\delta^{18}\text{O}$ versus $\delta^{13}\text{C}$) with analysis points grouped according to location and mineral (calcite, dolomite etc.). For the purposes of this diagram, data from the late carbonate encrustations have been plotted assuming they are smithsonite. For comparison purposes several additional fields are depicted: (i) A generalised burial diagenetic trend in carbonates (Choquette and James, 1987), (ii) Permo–Triassic diagenetic trends recorded in the Sellafield boreholes (Milodowski et al., 1998) and (iii) Burial related carbonate-hosted Pb–Zn mineralisation at Silvermines, Ireland (Reed and Wallace, 2004). The tie lines join analyses of different carbonate generations from the same samples.

crystals, finely crystalline saddle-shaped crystals (almost certainly ankerite) have been replaced by Fe–Mn-oxides (Figure 8c) indicating episodic precipitation of ankerite during fluorite precipitation and prior to oxidative alteration of the ankerite (see below). Under CL, the fluorite typically displays well-defined oscillatory concentric growth zoning with subordinate sector zoning. In addition, brecciated fluorite textures are commonly observed with re-cementation by fluorite with different luminescence character (Figure 8d).

Fluid inclusions in vein-lining fluorite have homogenisation temperatures that span a relatively narrow range (predominantly 100–120°C; Figure 5c and Figure 6). These temperatures are possibly slightly lower than those observed in the host rock dolomite and the fracture- and vug-lining ankerite. However, the fluids are of similarly high salinity (predominantly >19 wt% salt equiv.) with suppressed T_{fm} (–60 to –50°C) suggestive of mixed NaCl–CaCl₂-bearing brines as reported previously (e.g. Sawkins, 1966). Calculated NaCl/(NaCl + CaCl₂) ratios are typically in the range 0.60–0.75 (Figure 5b), although at the Hilton Mine fluoritic outlier, the fluids are typically more sodic in character, even though bulk salinities are comparable with those seen within the central fluorite zone. Some inclusions develop an additional K–Fe–Cl daughter phase on freezing (composition proved during microchemical analysis). The presence of dissolved cations in addition to Na and Ca

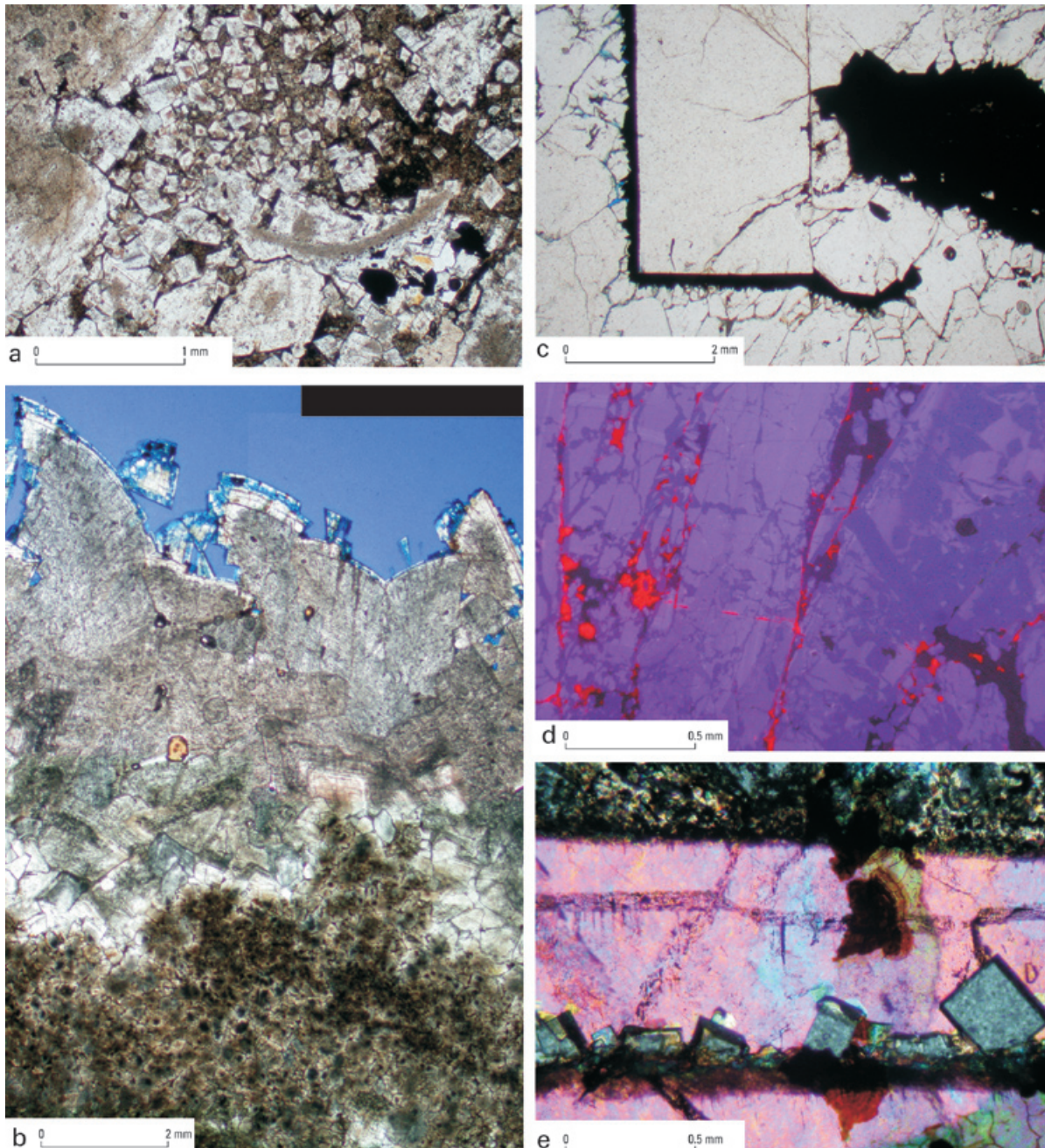


Figure 8 Representative photomicrographs of main ore and gangue-phases from stratabound mineralisation in the North Pennine Orefield.

- a** Dolomitised limestone, showing partial preservation of the outlines of bioclastic material. Dolomite crystals have inclusion-rich cores, and limpid overgrowths. (Sample from Small Cleugh Mine; PPL.)
- b** Dolostone at the bottom of the image contains finely crystalline, inclusion-rich rhombs. The vug-margin is highly irregular, and the earliest generation of dolomite growing into open pore space has euhedral morphologies and is relatively inclusion-free. The dolomite becomes progressively coarser-grained, more inclusion rich, and develops saddle-shaped crystals indicating increasing Fe content (ultimately to ankerite). The outermost generations are lightly corroded. Porosity filled with blue-dyed resin. (Sample from Small Cleugh Mine; PPL.)
- c** Detailed photomicrograph showing fluorite nucleated on an irregular core of (now oxidised) ankerite. The fluorite develops a well-defined euhedral form, which is marked by a break in fluorite precipitation, during which a thin band of ankerite developed. The ankerite has been subsequently replaced by Fe and Mn oxides. (Sample from Wellheads Hush; PPL.)
- d** Cathodoluminescence image of fluorite, showing subtle variations in luminescence colour between successive growth zones, and brecciation and recementation by later fluorite. This later fluorite is, in turn, brecciated and re-cemented by red-luminescent smithsonite. (Sample from Eastgate Cement Works Quarry.)
- e** Detail showing finely crystalline cubic euhedra (isotropic-grey) of fluorite at growth zones in quartz cement (pink birefringent). (Sample from West Rigg Open Cut; XPL.)

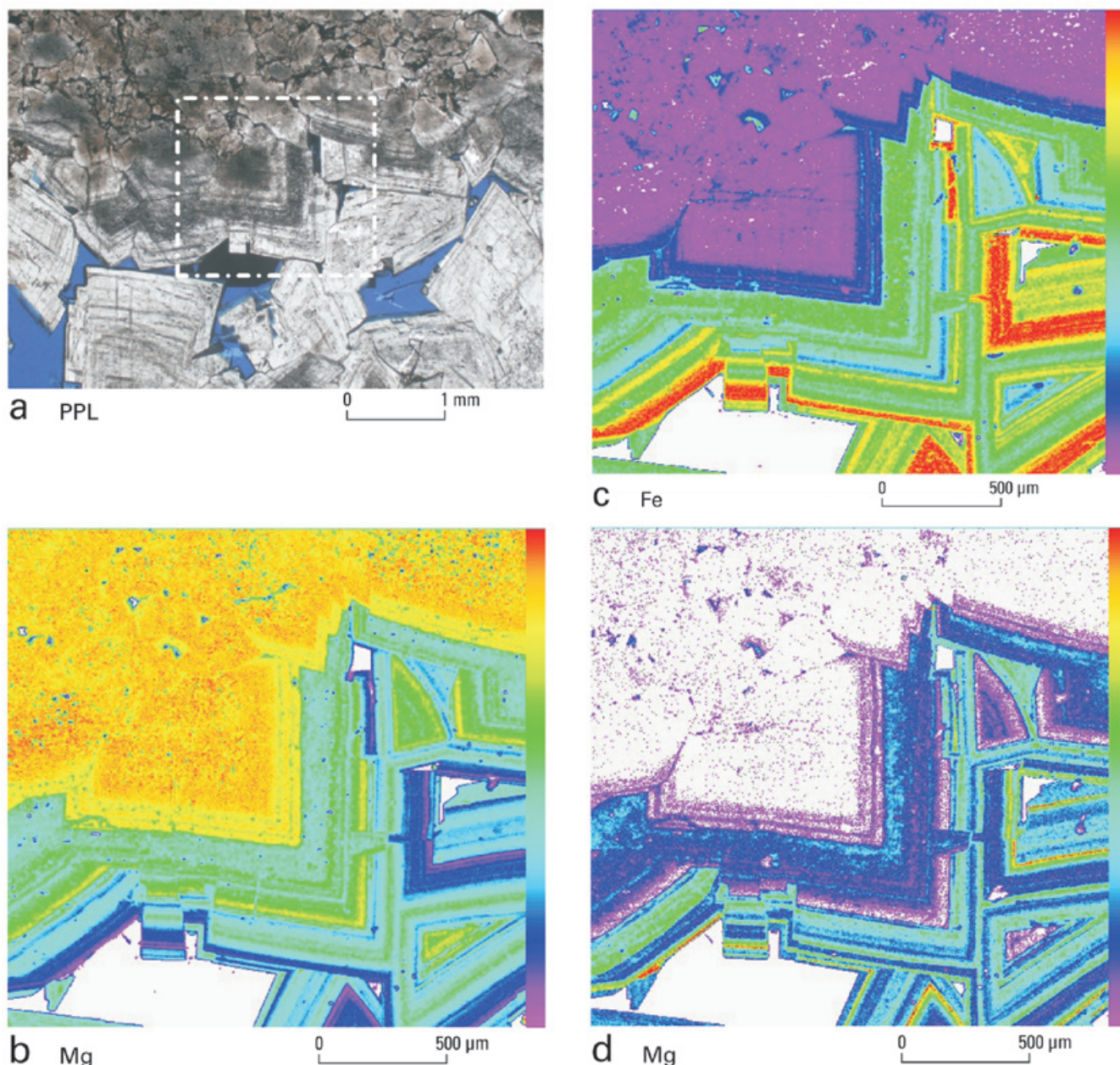


Figure 9 Compositional variations in zebra-dolomite developed during stratabound mineralisation in the North Pennine Orefield.

a Plane polarised light image, showing relatively finely crystalline, relatively inclusion-rich dolomitic host rock adjacent to margin of dm-scale vug (porosity impregnated with blue-dyed resin). The vug margin is lined by coarsely crystalline, relatively inclusion-free, ankerite. The boxed area is shown in more detail in **b**, **c** and **d** EPMA X-ray maps for Mg, Fe and Mn respectively, showing variations in chemistry between host rock dolomite, and successive generations of vug-lining ankerite. The scales at the right hand side of each image relate to the concentration of the element of interest, with brighter/warmer shades representing higher concentrations. (Sample from Small Cleugh Mine.)

is further confirmed by fluid inclusion microchemical analysis, with inclusions locally containing very high levels of dissolved metals, and in particular Fe (Fe up to 7100 ppm, Cu up to 350 ppm, Zn up to 1130 ppm and Pb up to 1200 ppm; Table 2). Such concentrations are very high compared to normal high TDS sedimentary brines. For example, Na–Ca–Cl brines encountered during drilling for hydrocarbons in the central and southern North Sea with similar TDS to the North Pennine inclusions, have typical Fe-contents of 50–300 ppm (Warren et al., 1994). K concentrations are relatively low (typically <7000 ppm), and Na:K ratios are correspondingly high (typically 10:1

to 15:1). These ratios are slightly higher than, but broadly comparable with, values recorded by Rankin and Graham (1988) for crush-leach analyses of fluorite.

In addition to the fracture- and vug-lining forms, fluorite also occurs, locally in association with quartz and/or chalcedony, as a metasomatic replacement of the limestone host rock, and also as a cement within saccharoidal dolostones. This replacement is most intensive at fracture/vug margins, and decreases in intensity over a distance of a few centimetres. Where the host rock is only incipiently dolomitised, fluorite crystals clearly engulf isolated dolomite euhedra, indicating formation after dolomitisation.

Table 2 Results of laser-ablation microprobe fluid inclusion microchemical analysis. Concentrations are determined relative to Na-concentrations, which are known from fluid inclusion microthermometric analysis. Analyses highlighted with a “*” were run using a dynamic reaction cell (see materials and methods section). n.a. = not analysed, n.d. = not detected, m.i. = matrix interference prevented concentration determination.

Sample	Location	Mineral	Sodium content (wt%) from micro-thermometry	Estimated Na (ppm)	Li (ppm)	K (ppm)	Mg (ppm)	Mn (ppm)	Fe (ppm)	Cu (ppm)	Zn (ppm)	Sr (ppm)	Ba (ppm)	Pb (ppm)	Na/K wt ratio			
NQ1040	Hilton Mine	Barite	5.0	50 000*	n.a.	40900	1100	n.d.	m.i.	m.i.	m.i.	m.i.	m.i.	m.i.	1.22			
				50 000*	n.a.	16600	500	n.d.	m.i.	3.01								
				50 000*	n.a.	37000	2100	n.d.	m.i.	n.d.	m.i.	m.i.	m.i.	m.i.	m.i.	1.35		
				50 000*	n.a.	40100	5900	m.i.	m.i.	1.25								
				50 000*	n.a.	20300	3900	m.i.	m.i.	2.46								
				50 000*	n.a.	35100	4800	600	m.i.	m.i.	1.42							
				50 000*	n.a.	37000	5600	n.d.	m.i.	m.i.	1.35							
				50 000*	n.a.	15800	m.i.	m.i.	m.i.	n.d.	m.i.	m.i.	m.i.	m.i.	m.i.	m.i.	3.16	
				50 000*	n.a.	32500	7600	m.i.	m.i.	m.i.	1.54							
				50 000*	n.a.	38200	10300	m.i.	m.i.	m.i.	1.31							
				50 000*	n.a.	4000	1100	300	m.i.	m.i.	m.i.	m.i.	m.i.	m.i.	12.50			
NQ1011	Rogerley Mine	Fluorite	6.5	65 000	320	5900	720	250	n.d.	n.d.	n.d.	660	2100	200	11.02			
				65 000	n.d.	4900	n.d.	n.d.	n.d.	n.d.	180	400	n.d.	n.d.	n.d.	13.27		
				65 000	200	4000	580	120	7100	350	m.i.	700	n.d.	n.d.	n.d.	16.25		
				65 000	220	4300	430	80	1200	10	10	350	140	n.d.	n.d.	15.12		
				65 000	n.d.	3800	830	n.d.	3600	110	n.d.	550	n.d.	10	n.d.	17.11		
						60 000	150	7000	1000	90	620	50	120	410	90	20	8.57	
						60 000	90	5700	1300	200	2400	180	450	360	770	1200	10.53	
						60 000	90	7200	1600	610	m.i.	310	1130	510	250	1200	8.33	
						60 000	1800	3500	900	100	n.d.	n.d.	n.d.	360	60	90	17.14	
						60 000	90	3000	300	n.d.	n.d.	n.d.	n.d.	270	70	n.d.	20.00	
NQ1021	Small Cleugh Mine	Quartz	7.75	75 000*	n.a.	5700	3400	130	1200	20	80	1500	190	60	13.60			
				75 000*	n.a.	18900	6100	m.i.	m.i.	n.d.	710	330	m.i.	470	4.10			
				75 000*	n.a.	22500	1400	60	m.i.	n.d.	40	2200	70	30	3.44			
				75 000*	n.a.	17800	m.i.	m.i.	m.i.	50	m.i.	m.i.	m.i.	n.d.	4.35			
				75 000*	n.a.	5000	400	70	80	n.d.	20	820	60	20	15.50			
				75 000*	n.a.	6100	1700	100	590	n.d.	140	1300	60	60	12.70			
				75 000*	n.a.	6200	1500	20	870	n.d.	40	560	40	n.d.	12.50			
				75 000*	n.a.	24200	1200	40	170	n.d.	20	1200	90	10	3.20			

2.3.6 Quartz

This predominantly occurs as coarsely-crystalline (cm-scale) euhedra, which in some locations engulf fluorite and in others are engulfed by fluorite. There are also examples of repetitive cycles of fluorite-quartz-fluorite mineralisation (Figure 8e), inclusions of fluorite trapped on growth zones within quartz crystals, and of finely-crystalline quartz-fluorite intergrowths at the transitions between quartz and fluorite crystals. All these features are indicative of episodic or cyclic precipitation of fluorite-dominated and quartz-dominated assemblages.

As might be expected, given their overlapping parageneses, fluid inclusions in quartz have very similar salinities (>18 wt % salt equiv.) to those seen in the fluorite. However, the fluids are typically more sodic (calculated NaCl/

(NaCl+CaCl₂ peak at 0.70–0.80; Figure 5b). This variation is also reflected in the microchemical analyses, with inclusions in quartz typically having lower Fe, Cu, Zn and Pb contents and higher Mg and Sr contents than inclusions in fluorite (Table 2). K concentrations are variable. Some inclusions have Na:K ratios comparable to those seen in fluorite (approximate range 10:1 to 20:1), whereas others have low Na/K ratios (approximate range 3:1 to 5:1), with a closer affinity to inclusions seen in barite (see below).

Within the quartz, there is also a small, but significant, population of relatively low-salinity inclusions (<10 wt% salt equiv. Figure 5a and Figure 6). Inclusions with similarly low salinities have been reported on the margins of the orefield where they occur exclusively within barite (Cann and Banks, 2001). However, fluids with these

relatively low salinities have not been previously reported in the central fluorite zone. Homogenisation temperatures are slightly more variable (typically 90–130°C; Figure 5c) than observed in fluorite, and there is also a significant population of monophase inclusions which, as discussed above, probably represents inclusions containing stretched fluids from the low temperature end of the T_h frequency distribution. The presence of this monophase population may indicate that, although homogenisation temperatures of fluorite and quartz are comparable, quartz precipitation continued at lower temperatures than those that prevailed during fluorite precipitation. There is no relationship between inclusion type (monophase versus 2-phase) and inclusion salinity. Minor amounts of quartz and chalcedony are also present as microcrystalline encrustations on vein and vug surfaces that tend to coarsen outwards and, where space permits, develop into more coarsely crystalline euhedra.

2.3.7 Sulphides

A description of the full range of sulphide minerals and their relationships is outside the scope of the present study, but summaries of the sulphide mineralogy within the main veins can be found in Vaughan and Ixer (1980) and Dunham (1990). The sulphide mineralogy of the stratabound mineralisation studied here is dominated by galena and sphalerite although minor pyrite and chalcocopyrite are also noted. Sulphides occur predominantly as vein or vug-filling euhedra, which appear to be paragenetically related to the development of fluorite. Minor amounts also occur as cements in the wall rocks adjacent to fractures. There are numerous examples of sulphide precipitation beginning approximately coeval with the onset of fluorite precipitation. However, sulphide precipitation stopped before fluorite, and consequently the sulphides are engulfed by later generations of fluorite. As was described for fluorite, where galena occurs within partially dolomitised host rocks, sulphides engulf planar-euhedral isolated dolomite rhombs indicating that sulphide precipitation was post-dolomitisation. Limited fluid inclusion data derived from sphalerite indicates high salinities for this fluid (21–23 wt% NaCl equiv.) with highly variable homogenisation temperatures (80–150°C; Figure 5c and Figure 6).

2.3.8 Calcite

Relatively minor amounts of irregular calcite veining are associated with the mineralisation. This tends to occur as cement within brecciated domains and is characterised by notably higher Fe- and Mn-contents (0.01–0.03 and 0.02–0.06 formula units respectively; Figure 4), and lower Mg contents (typically <0.01 formula units) than those

of the calcite in both the host rocks and also in the later generations of supergene calcites.

2.3.9 Barite

This mineral has only been observed from Hilton Mine, where it forms coarse radial bundles of tabular crystals that engulf vug-lining, euhedral fluorite. Fluid inclusion data indicate generally lower salinities than observed in other minerals, and the inclusions are overwhelmingly monophase, indicating relatively cool conditions during precipitation. However, T_{fm} is low (c. –55°C) suggesting that a mixed NaCl–CaCl₂-brine was responsible for barite precipitation. Due to chemical interference from the barite host, it proved impossible to acquire meaningful microchemical data on the trace metal contents of inclusions in barite. However, Na:K ratios are much lower than in the fluorite (typically 1:1 to 3:1; Table 2), and are similar to those of highly evaporated marine waters precipitating halite (Timofeeff et al., 2001). The Mg contents are lower than for unmodified marine brines, but this is to be expected since Mg is quickly lost from solution by mineral–fluid interactions, especially in carbonate host rocks.

We have no new stable isotope data for barite. However, published $\delta^{34}\text{S}$ and $\delta^{18}\text{O}_{\text{SMOW}}$ data suggest a source in lower Carboniferous anhydrite, which is present in the adjoining Northumberland–Solway Basin (Solomon et al., 1971; Solomon et al., 1972; Crowley et al., 1997). Values of $\delta^{18}\text{O}_{\text{SMOW}}$ are predominantly between 10 and 15‰ and, assuming barite crystallisation occurred at relatively low temperatures (c. 50°C) as suggested by the monophase nature of the fluid inclusions, this equates to a fluid with $\delta^{18}\text{O}_{\text{SMOW}}$ in the range –13 to –7‰ (using the fractionation factors of Friedman and O’Neil, 1977), which is notably lighter than our data for dolomite and ankerite.

2.3.10 Late carbonates

Euhedral, coarsely crystalline calcite is locally developed on the earlier minerals, and encrustation by finely crystalline calcite is common. In terms of Fe, Mn and Mg contents, these calcites are indistinguishable from those in the host rocks. However, they locally contain well-developed fine-scale growth zones containing notably high concentrations of Pb and/or Zn (EPMA analyses show concentrations of up to 4.1 wt% PbO and 1.3 wt% ZnO). In addition, all the minerals described above may be overlain by typically mm-thick encrustations of very fine-grained or scaly carbonates, which appear uniformly white or cloudy in hand specimen. EPMA, SEM and CL analysis reveals a mixture of strongly red and blue luminescent smithsonite, green-luminescent cerussite and other unidentified mixed Si–Mn–Pb–Zn-bearing phases. No fluid inclusion analyses were possible on these carbonates due to their scaly character.

3 Discussion

3.1 MECHANISMS OF POROSITY GENERATION

The bulk of the mineralisation within the North Pennine Orefield is well-understood as an excellent example of fracture-hosted mineralisation, with open fractures within 'hard beds' hosting much of the mineralisation in the main vein system (Dunham, 1990). However, field and petrographical evidence suggests that, rather than representing exclusively metasomatic replacement of limestone host rocks, the stratabound mineralisation also occurred in a structurally active setting, in which brecciation of earlier-formed minerals and re-cementation by successive mineral generations was common (Figure 10a). In addition, as a significant proportion of the North Pennine stratabound-style mineralisation is hosted in vuggy porosity. It is important to establish whether the mineralisation exclusively exploited pre-existing pore space, or was accompanied by porosity generation and redistribution, hydrothermal karstification, where the karst-forming process and the mineralisation should be contemporaneous (Sass-Gustkiewicz et al., 1982; Leach et al., 1996; Sass-Gustkiewicz, 1996). Lines of evidence for this include the presence of internal clastic sediments (possibly comprising reworked fragments of earlier formed hydrothermal minerals) intimately interbedded with chemical sediments, and collapse breccias containing mineralised fragments which are themselves recemented by later ore minerals. The following features provide some constraints on the relationships between dissolution of the host rocks, their dolomitisation and their mineralisation:

1 MINERALISED BRECCIAS Generations of earlier mineralisation are commonly brecciated and recemented by later generations of mineralisation (Figure 10a). In addition, there are also examples where fluorite-cemented breccias contain individual clasts of dolostone, which carry euhedral ankerite (now replaced by supergene Fe-oxides) indicative of growth into open space, along only one of their surfaces. It would seem highly unlikely for ankerite to precipitate on only one surface of a breccia clast, and therefore, this ankerite is interpreted to have precipitated at the margins of vugs within a dolostone, prior to brecciation and subsequent mobilisation.

2 INTERNAL SEDIMENTS These are typically poorly represented. However, laminae (1–2 mm thick) of fine-grained sediments can line mineralised cavities. In all cases the sediments comprise a mixture of rhombs of oxidation products of ankerite (Fe and Mn oxides), and irregular fluorite and quartz crystals, which are cemented by finely crystalline quartz and fluorite (Figure 10d). These sediments display faint internal lamination, and thicken into the irregular surfaces of the fracture or vug margins (Figure 10c). The contemporaneity of the sediment relative to the mineralisation is demonstrated by an example where the sediment lies on top of a fracture or vug-coating of highly brecciated fluorite, and is overlain by coarsely crystalline fluorite cement (Figure 10b).

3 PRESERVED FRACTURES WITHIN VUGS Mineralised fractures are locally preserved where dissolution has removed the

surrounding host rock (Figure 3f) prior to cementation by later mineralisation. This indicates that some fracturing and mineralisation occurred prior to dissolution, but that mineralisation continued after dissolution.

4 MINERALISED VUGS Vugs occur at a range of scales (cm to m), and are typically elongate parallel to bedding in dolomitised host rock. In some cases they were clearly developed following an earlier episode of fracturing and cementation. Within the host rock, dolomite is inclusion-rich with idiotopic-subhedral morphologies. The earliest generations of vug-lining dolomite are inclusion-poor with idiotopic-euhedral morphologies clearly indicative of growth into open space. The margins of the vugs, as defined by the contact between the inclusion-rich and the inclusion-free dolomite, have irregular geometries which are highly unlikely to have been generated by fracturing (Figure 3g and Figure 8b). However, it is common for an individual dolomite crystal to straddle this contact with an inclusion-rich portion of replacive character within the host rock, and an inclusion-free portion growing into open space. In addition, the earliest generations of vug-lining dolomite or ankerite are commonly indistinct from the dolomite within the host rock in terms of both minor element and fluid inclusion chemistry. These features suggest that the formation of the vuggy porosity to large extent, predates or is coeval with dolomitisation of the wall rocks, the more ferroan/manganoan carbonate mineralisation, and the main fluorite–quartz–sulphide mineralisation. However, the absence of vuggy porosity within undolomitised limestones suggests that whilst dissolution largely predates dolomitisation, the two processes are somehow related.

5 ZEBRA DOLOMITES These probably represent a special case of the mineralised vugs as described above. The formation of zebra dolomites is considered to be an essentially two-stage process (Wallace et al., 1994; Nielsen et al., 1998). It begins with the development of a sheeted porosity system within the host sediments, in this case limestone, initiated by fracturing and/or dissolution. This is followed by coeval replacement of the host rock and cementation by ore-stage minerals, such as dolomite and ankerite. At the sites examined in the North Pennine Orefield, zebra dolomites are by no means as abundant or as well-developed as those described by Arne and Kissin (1989), Wallace et al. (1994) Nielsen et al. (1998) and Boni et al. (2000). However, at Small Cleugh Mine, where mineralisation occupied over $3 \times 10^6 \text{ m}^3$, they are particularly well-developed (*see* Dunham, 1990; p.149, Plate 3) and their mode of formation can be deduced. The contacts between the white and black zebra dolomite sheets are, in detail, irregular and commonly lobate rather than planar. This suggests that they represent dissolution voids or fractures enhanced by dissolution, rather than simple fractures. Features of the zebra dolomites seen in North Pennine stratabound mineralisation are consistent with those described in the studies cited above. These include their general textures, the similarity in composition and fluid inclusion characteristics (salinity, modelled dissolved components and homogenisation temperatures) between the

dolomite host rock and the earliest generations of dolomite or ankerite cements, and the indistinct nature of the contact between the black dolomite and the white dolomite or ankerite sheets when viewed in detail.

Features 1 to 3 suggest that pore-system development and modification could to some degree be ascribed to processes of hydrothermal karstification, with some earlier-formed minerals being remobilised into breccias and internal sediments prior to cementation by later generations of minerals. A degree of carbonate wall-rock dissolution would be expected in response to the reduction in fluid pH that would occur as metal sulphides are precipitated from a chloride-rich solution. However, features 4 and 5 seem to suggest that a significant proportion of the vuggy porosity was generated prior to, or coeval to, significant dolomitisation. Since the dolomitisation is paragenetically early, most porosity generation must predate the bulk of fluorite–quartz–sulphide mineralisation. In the cases of features 4 and 5, whereas there is a great degree of similarity between the host rock replacive dolomite and the earliest generations of vug-filling dolomite or ankerite, the volumetrically more significant, later generations of vug-filling dolomite or ankerite have distinctive minor element and isotopic compositions. These are discussed further below.

3.2 HISTORY OF MINERALISATION

3.2.1 Burial diagenesis

Petrographical examination of the undolomitised and unmineralised limestones failed to reveal any features consistent with early (i.e. marine) diagenetic processes. However, fluid inclusions in calcite cements are of notably lower salinity than those observed within the paragenetically later replacive and fracture-lining dolomite or ankerite and the fluorite and quartz associated with the main mineralisation. The majority of inclusions have salinities of between 2 and 6 wt% NaCl equiv. and have T_{fm} consistent with a NaCl-dominated fluid, suggesting that this fluid might represent slightly evolved sea-water. CL and EPMA both indicate low Fe and Mn concentrations, but relatively high Sr concentrations in the calcite, which are also consistent with a sea-water derivation for this fluid. Whereas Mg contents are higher in the calcite cements relative to calcite related to later mineralisation and supergene alteration, they are low (predominantly less than 0.5 wt% MgO) relative to marine diagenetic high-Mg calcites that might be expected to contain several weight % MgO (Tucker and Wright, 1990). The stable isotope data from host rock calcites indicate relatively light $\delta^{18}\text{O}$ compositions ($\delta^{18}\text{O}_{\text{PDB}}$ of -12.2 to -5.7‰) compared with those from Carboniferous marine brachiopods ($\delta^{18}\text{O}$ typically between -3 to -8‰ PDB, Bruckschen and Veizer, 1997). The presence of appreciable Sr, but the absence of cement textures indicative of marine diagenesis, suggests that later diagenetic processes have significantly overprinted any marine diagenetic signatures. Fluid inclusion data suggest that this was probably due to interaction with slightly modified (concentrated) sea-water, with slightly elevated temperatures during burial responsible for the lighter $\delta^{18}\text{O}$ signatures (Figure 11a). The broad range observed in Th for calcite cements (75–160°C) may indicate some leakage of the inclusions in response to later heating during dolomitisation and mineralisation, and the presence of some high salinity inclusions (up to 12 wt% salt equiv.) may also reflect overprinting by later fluids.

3.2.2. Vuggy porosity generation and dolomitisation/ankeritisation

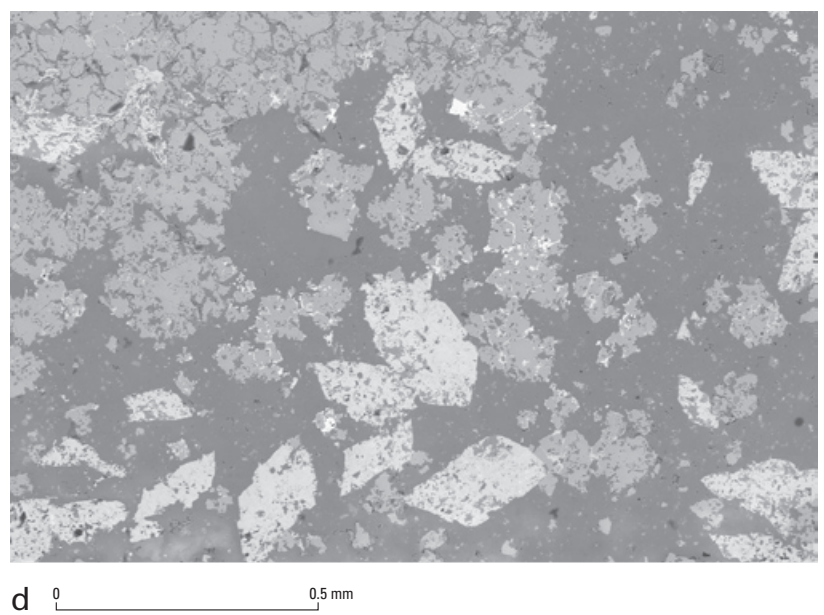
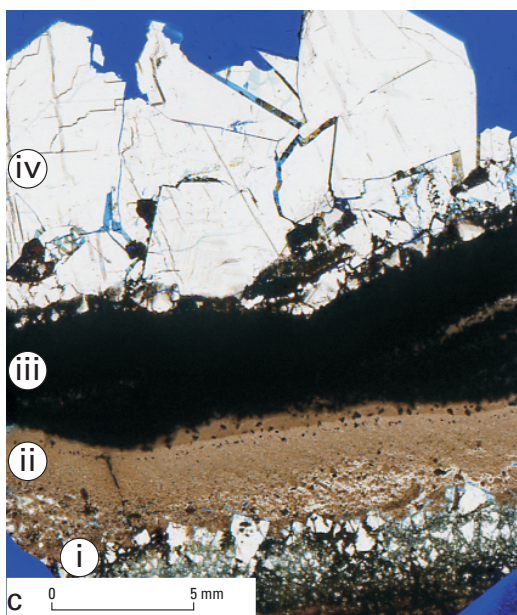
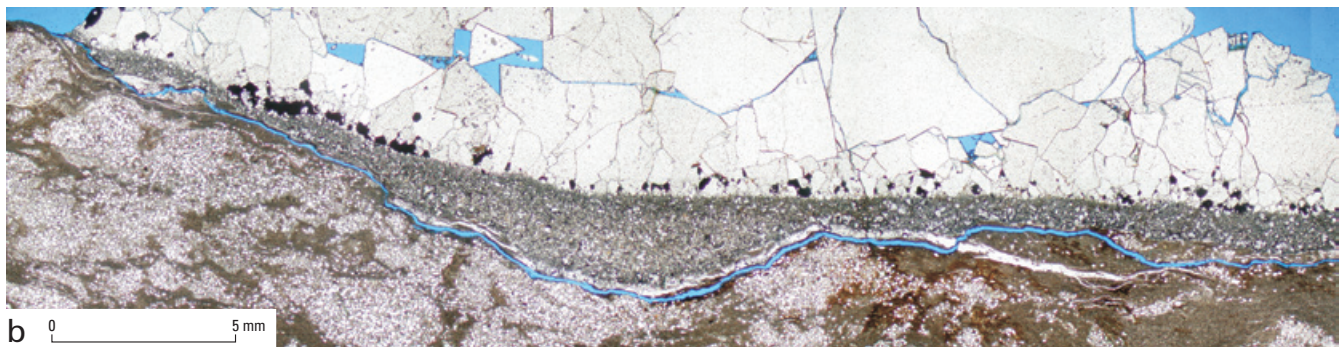
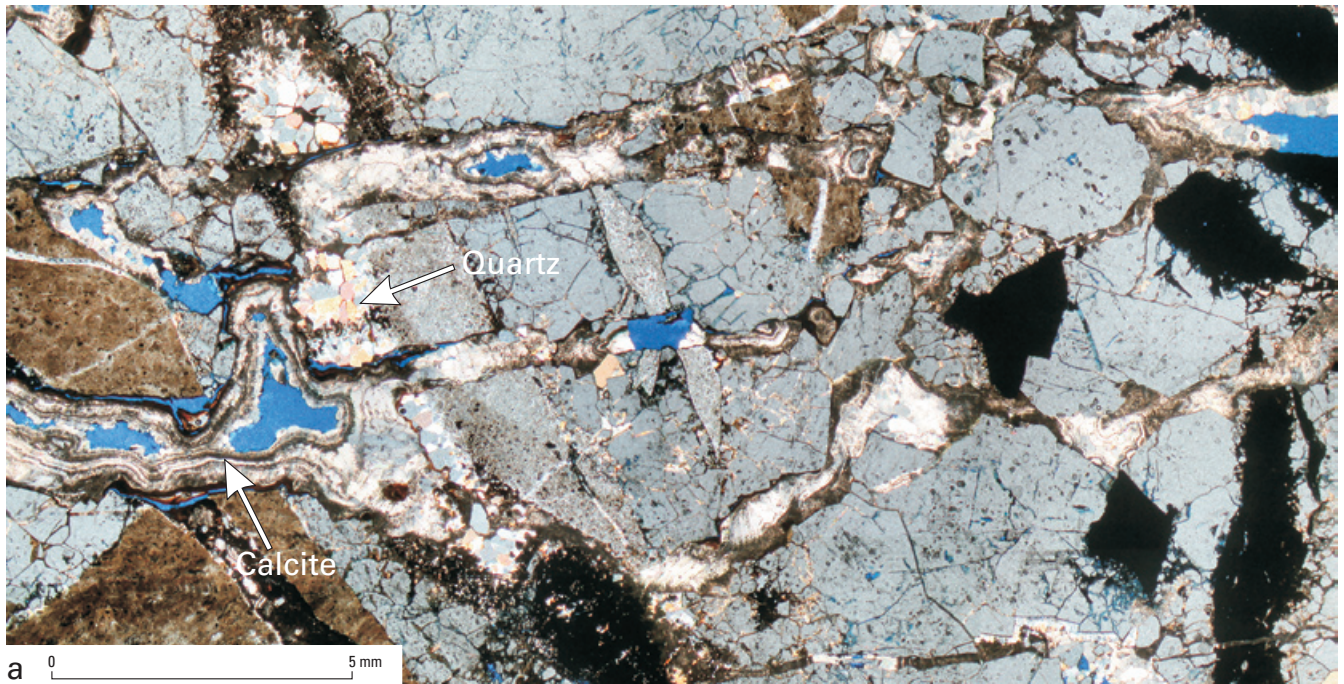
There is evidence to suggest that, whilst porosity generation and modification occurred throughout mineralisation, generation of significant vuggy porosity was somehow related to dolomitisation of the host rocks, which is widely accepted to be variably generative, conservative, or destructive of porosity, depending upon the precise mechanism of dolomitisation (Purser et al., 1994). Models of mixing between brine and a low salinity groundwater in carbonate host rock (Corbella et al., 2004) appear to provide a satisfactory explanation for the observed redistribution of porosity during subsequent mineralisation.

Wall-rock replacive dolomite and the earliest generations of vuggy- and fracture-lining dolomite are indistinguishable both in terms of fluid inclusion salinities (c.20 wt% salt equiv. CaCl₂–NaCl-brines; Figure 5) and minor element chemistry. However, fluid inclusion homogenisation temperatures for ankerite extend to both higher and lower temperatures than observed in the wall rock dolomite. Furthermore, as precipitation progresses, dolomite compositions become progressively more ferroan, manganous and isotopically lighter ($\delta^{18}\text{O}$).

The chemical variations indicate either a progressive shift in fluid composition to higher Fe- and Mn-contents and/or a change in pH and/or Eh conditions such that Fe²⁺ and Mn²⁺ progressively became the dominant dissolved iron and manganese species. Given the absence of hematite associated with the earlier dolomite generations, which would be consistent with oxidising conditions and a Fe-rich pore-fluid, a shift in Eh seems unlikely. In a study of calcite cements on the South Derbyshire platform, Hollis and Walkden (1996) reported a similar increase in calcite Fe and Mn contents as mineralisation progressed, which they attributed to progressive clay-mineral transformations in the adjacent basins filled with Namurian shales, most notably the illite–smectite transition, which releases Fe and Mn (Boles and Franks, 1979) and the reduction of Mn-oxide coatings (Francois, 1988).

Figure 10 (opposite) Features of brecciation, internal sediments and mineralised vugs.

- a** Coarsely crystalline fluorite (grey) is extensively brecciated and recemented by patches of quartz (arrowed) and later finely crystalline, banded calcite (arrowed). (Sample from West Rigg Opencut, XPL).
- b** Detailed photomicrograph of a siltstone host rock with an irregular surface upon which are deposited finely laminated internal sediments which thicken into the hollows. On top of the internal sediment are developed finely crystalline galena euhedra (opaque, black), which are engulfed by fluorite (white). A thin smithsonite vein exploits the plane of weakness between the host rock and the internal sediment (Sample from Hilton Mine, PPL).
- c** Scan of polished thin-section showing (i) a relatively early substrate comprising brecciated fluorite. On top of this is developed (ii) a finely cross-laminated internal sediment (*see d* for more detail). This is overlain by (iii) a band of opaque oxidised ankerite, and finally by (iv) coarsely crystalline fluorite. (sample from Eastgate Cement Works Quarry).
- d** BSEM detail of c, showing the internal sediment consisting of skeletal fragments of fluorite (mid grey) and ankerite (light grey; replaced by Fe and Mn oxides) in a quartz/silica cemented matrix (dark grey). (Sample from Eastgate Cement Works Quarry).



Paired analyses of pore-filling dolomite/ankerite and host rock dolomite indicate that the oxygen within the pore-filling dolomite/ankerite is isotopically lighter by 3–7‰ (Table 1). Progressively lighter oxygen isotope

compositions of burial diagenetic carbonate cements are typically attributed to progressive increases in temperature of mineral precipitation (e.g. Choquette and James, 1987). According to this interpretation, the degree of

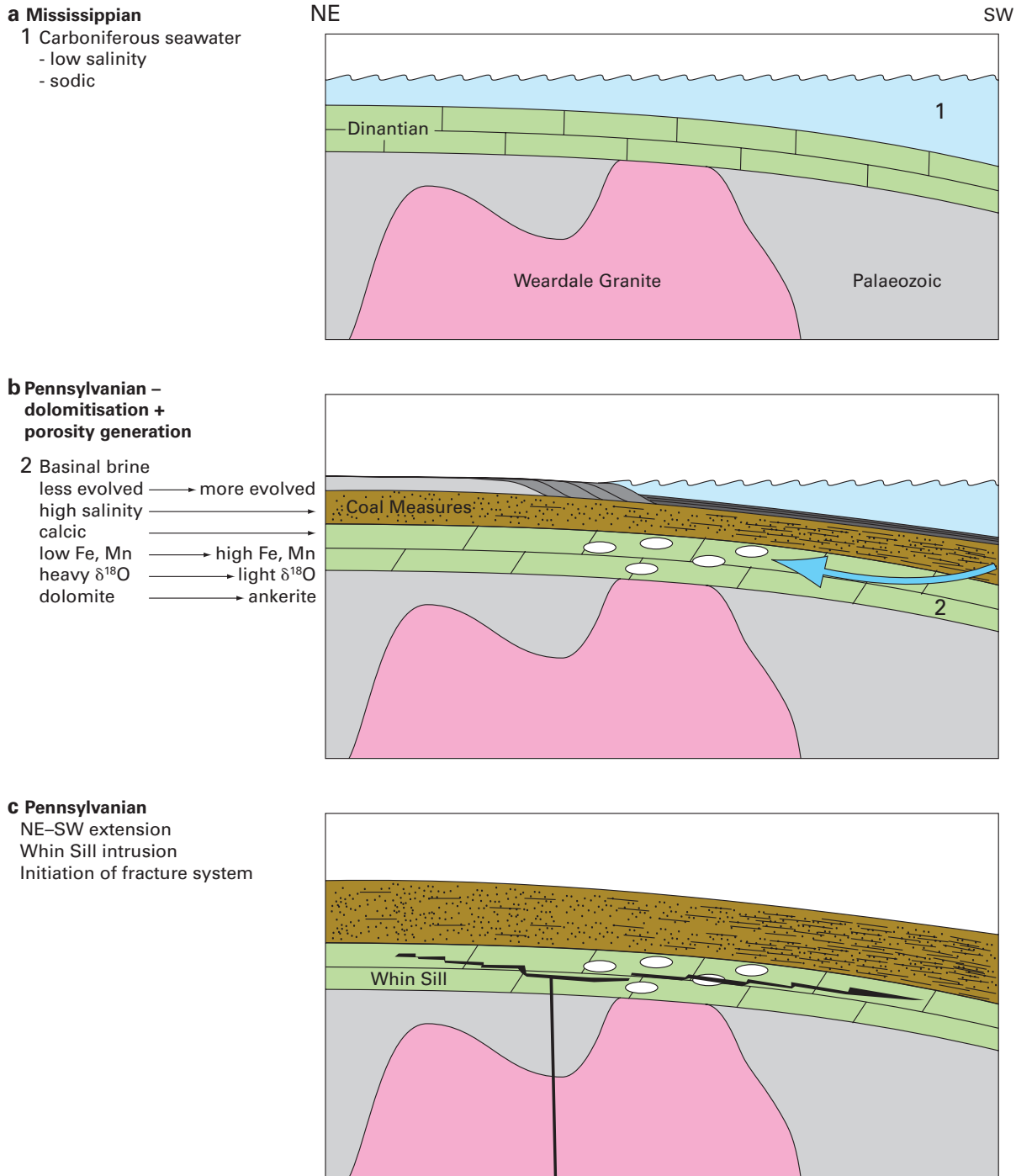


Figure 11 Summary diagram illustrating the evolution of the North Pennine Orefield from Lower Carboniferous through to Triassic times.

isotopic variation seen here would imply an increase in mineralisation temperatures of about 50°C between the dolomite and the ankerite precipitation. Whereas the T_h data for ankerite extend to higher temperatures than those seen in the wall-rock dolomites, the data suggest that precipitation of host rock dolomite and fracture- and vug-filling ankerite, including zebra dolomites, occurred at similar temperatures (T_h around 110–130 °C; Figure 5), so a temperature increase of the magnitude suggested by the stable isotope data is not supported. A change in the isotopic composition of the fluid is therefore a more likely explanation. This is supported by the $\delta^{13}\text{C}$ data, which possibly reflect an increased component of CO_2 from organic compounds possibly related to increased hydrocarbon maturation in the source

rocks, although no hydrocarbons have been observed within our samples.

The observed chemical and isotopic variations are both consistent with the ankerite precipitating from a fluid of more evolved character than that responsible for dolomitisation. Therefore, we consider that the dolomitising and ankerite-precipitating brines were expelled from progressively maturing basinal shales, possibly over a period extending from the late Carboniferous into the early Permian (Figure 11b). The high levels of Fe and Mn observed within the later generations of ankerite, may have been sourced from the interaction with the Whin Sill (Dunham, 1948; Ineson, 1968) and/or the Weardale Granite (which in places contains finely divided hematite) during

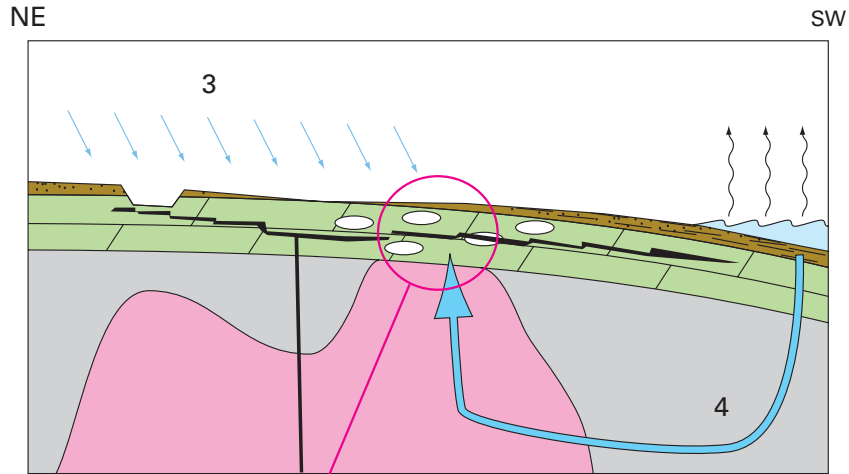
d Permian – fluorite-quartz-sulphide mineralisation

3 Meteoric water

- low salinity
- low Na:K
- low sulphate

4 Evaporated brine

- high salinity
- high Na:K
- dense
- deep circulation adds:
heat + metals + F



Fluorite-quartz-sulphide mineralisation initiated by mixing of fluids 3 and 4

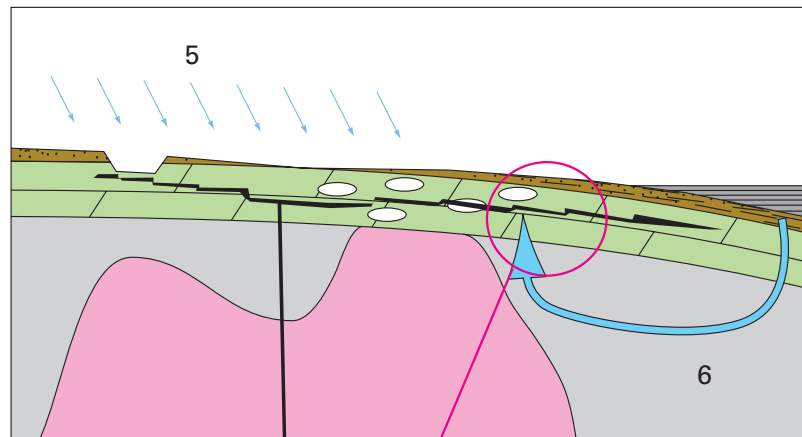
e Triassic (?) – barium mineralisation

5 Meteoric water with dissolved evaporates

- low salinity
- low Na:K
- high sulphate

6 Evaporated brine

- reduced salinity
- waning circulation
- reduced metal content
- reduced temperature



Barium mineralisation initiated by mixing of fluids 5 and 6

Figure 11 *continued.*

the early stages of hydrothermal circulation in response to extension and fracturing initiated during late Carboniferous times.

3.2.3 Fluorite–quartz–sulphide mineralisation

Mineralised breccias and internal sediments provide evidence for continued modification and enhancement of the existing fracture and vuggy pore system during mineralisation in response to both fracturing and dissolution. Fluid inclusion data indicate that this mineralisation occurred in the presence of a fluid of similar character to that responsible for the bulk of the ankerite precipitation, under similar temperature conditions. Fluid inclusion homogenisation temperatures for fluorite, quartz and sphalerite are predominantly in the range 100–130°C. Salinities are high (mainly >19 wt% equiv.), and the fluid is interpreted as a mixed CaCl₂–NaCl–

bearing brine, which also contains significant amounts of dissolved Fe, Cu, Zn and Pb.

For the purposes of comparison, fluid inclusion data related to fluorite (predominantly Th data), with lesser amounts of data from barite and quartz, from the main vein mineralisation have been compiled from various PhD theses (Smith, 1974; Moore, 1980; Christoula, 1993; and Shepherd, unpublished), and plotted in Figure 5 ('legacy data') alongside our new data. Most of the published fluid inclusion data from the North Pennines have been presented as summary tables and diagrams (e.g. Sawkins, 1966; Shepherd et al. 1982; Dunham, 1990; Cann and Banks, 2001), in some cases without the nature of any pressure corrections applied being stated, making direct comparison of data difficult or unreliable. However, the legacy data suggest fluorite precipitation at temperatures in excess of 140°C, and quartz over the range 120–200°C.

On the basis of the legacy fluid inclusion data, mineral (Vaughan and Ixer, 1980) and alkali (Rankin and Graham, 1988) geothermometry and Eu-anomalies in fluorite (Shepherd et al., 1982; Bau et al., 2003), the general consensus is that mineralisation occurred from fluids with initial temperatures of at least 220°C (e.g. review in Ixer and Vaughan, 1993). Our data from the stratabound mineralisation suggest slightly cooler temperatures, with most inclusions in fluorite and quartz having homogenisation temperatures markedly lower than those recorded in the main veins. The presence of a significant population of monophasic inclusions in quartz reinforces this interpretation.

Our data also record a small component of a relatively low-salinity fluid present within the quartz, and to a lesser extent within the fluorite. To our knowledge, this low-salinity component has not been detected previously in direct association with the main fluorite mineralisation, although a low-salinity fluid associated with the barite mineralisation reported by Cann and Banks (2001), is also observed within our data (*see below*). The presence of this low-salinity component, coupled with the marginally more sodic nature of the fluids within the quartz cements compared with fluorite, suggests that mineralisation occurred when a very high salinity, relatively calcic, brine mixed with a lower salinity sodic brine. This is consistent with the models suggested by both Solomon et al. (1971) and Cann and Banks (2001), where ascending fluoride-rich, metalliferous brines mix with surficial or connate brines. The fact that direct evidence for the low-salinity fluid is preserved in the stratabound mineralisation, but has not been previously reported in the main vein mineralisation, may not be surprising. This is because the stratabound mineralisation can be distal relative to the fault-controlled migration pathways of the mineralising fluid and might, therefore, be expected to retain a greater signature of the pre-mineralisation pore fluids. Furthermore, the preferential preservation of the low-salinity fluid, coupled with the more sodic compositions of the inclusions in quartz, suggest that this mixing may be particularly important in quartz cementation, possibly reflecting the waning stages of individual influxes of metalliferous brines. This interpretation is also supported by the fluid inclusion microchemical data, with inclusions in fluorite having variable but elevated levels of metals, whereas those in quartz are significantly lower. We suggest that the sources of the two fluids (Figure 11d) are:

- 1 the low-salinity component possibly represents groundwater that percolated through the Carboniferous sediments during latest Carboniferous and Permian unroofing of the North Pennine Orefield.
- 2 the high-salinity component could be derived from dense evaporated brines generated during the Late

Permian in the adjacent Zechstein Sea and Vale of Eden Basins as suggested by Cann and Banks (2001). Cann and Banks (2001) also suggested that a major factor which governed the timing of the mineralisation was the restriction of high-salinity brines to late Permian times. As postulated by Cann and Banks (2001), these brines would have percolated to great depth through fractures generated during Permian extension, and into a hydrothermal convection cell associated with the production Weardale granite. At depth, the fluids could become heated and might be expected to react with both the Palaeozoic basement and the granite along their flow paths, which probably accounts for their high fluorine and metal contents (the Weardale Granite contains finely disseminated hematite where it is unaltered), before being driven back upwards into the fracture system above the granite where mixing and mineralisation occurred.

3.2.4 Barite mineralisation

Evidence from Hilton Mine indicates that barite mineralisation occurred under slightly different conditions from those responsible for the main fluorite–quartz–sulphide mineralisation. The predominance of monophasic inclusions within the barite suggests cooler precipitation temperatures. Furthermore, the fluid was of lower bulk salinity and characterised by lower Na:K ratios, comparable with those of highly evaporated marine waters (Timofeeff et al., 2001). A similar situation was described in the nearby Sellafeld area (Milodowski et al., 1998), where barite is isotopically ($^{87}\text{Sr}/^{86}\text{Sr}$ and $\delta^{34}\text{S}$) distinct, and contains inclusions of notably lower salinity and lower T_h than those of paragenetically related carbonates. Solomon et al. (1971) suggested that the stable isotope data from the barite in the North Pennine Orefield are consistent with sulphate derived from Triassic brines or Carboniferous sea-water, but ruled out Triassic brines on the basis of the likely timing of the mineralisation. Crowley et al. (1997) provide isotopic evidence for lower Carboniferous evaporites in the Northumberland–Solway Basin being a potential source of barite sulphur in both the North Pennine Orefield and the English Lake District. However, more recent interpretations of the timing of North Pennine Orefield mineralisation place it as Late Permian to Triassic in age, which would remove the objections of Solomon et al. (1971) to Triassic brines as a potential source of sulphate.

The lower temperatures, and salinities of fluid inclusions in barite relative to inclusions in fluorite and quartz possibly indicate that this represents the waning stages of hydrothermal circulation, possibly under slightly cooler conditions when the sources of metals within the basement and/or igneous intrusions had become depleted (Figure 11e).

4 Conclusions

The North Pennine Orefield records a complex history of mineralisation in response to changing fluid and tectonic conditions. In general terms, our data for the stratabound mineralisation are consistent with the model of Cann and Banks (2001), with the main mineralisation initiated by the availability of high-salinity fluids during Late Permian times, which were able to exploit an open fracture and vuggy porosity system generated due to extension and fracturing during latest Carboniferous times, leading to the development of an active hydrothermal cell, and ultimately mineralisation when this fluid mixed with groundwater. However, using new petrographic, stable isotope and fluid inclusion data derived from stratabound mineralisation adjacent to several veins, we are able to offer a significant refinement of this model. Our data allow us to recognise three main episodes of mineral precipitation: 1) dolomitisation and subsequent ankeritisation, 2) main quartz–fluorite–sulphide mineralisation and 3) barite mineralisation. Furthermore, we can provide some constraints on the likely sources of the different fluids, which changed over the evolution of the system.

The vuggy porosity, which hosts a large proportion of the stratabound mineralisation, was largely developed due to processes related to dolomitisation and ankeritisation. Wallrock dolomite and vug- and vein-lining ankerite are paragenetically early, and record a progressive increase in Fe and Mn contents and a decrease in $\delta^{18}\text{O}$ and $\delta^{13}\text{C}$ signatures indicating the involvement of progressively more evolved fluids that have probably experienced a greater degree of water-rock interaction. These features, coupled with the high Fe and Mn concentrations required to generate the observed ankerites, are all consistent with the dolomitising and ankerite-precipitating fluids representing progressively more evolved fluids that were expelled from the adjacent mud- and shale-filled basins. Fe and Mn contents may have been enhanced by interaction with the Whin Sill and/or the Weardale Granite during the early stages of hydrothermal circulation. The fluorite–quartz–sulphide mineralisation, was probably emplaced during the late Permian when high salinity brines from the evaporitic Zechstein Sea and Vale of Eden Basin were available (Cann and Banks, 2001).

In addition to representing passive replacement of host rocks, the stratabound mineralisation is commonly

accompanied by brecciation and dissolution, including the identification of features consistent with hydrothermal karstification (including mineralised breccias and internal sediments which lie on top of earlier mineralisation). Furthermore, there is evidence for brecciation and re-cementation by successive generations of mineralisation. Therefore, the mineralising fluids were also responsible for a degree of porosity modification and redistribution as carbonate host rocks were dissolved and the resulting vugs were cemented by fluorite. Recent modelling by Corbella et al. (2004) provides a likely mechanism for this process.

As observed in the main vein mineralisation, there is no simple paragenetic sequence observed for the quartz–fluorite–sulphide mineralisation and repeated cycles of fluorite-dominated, quartz-dominated and sulphide-dominated mineralisation occur. The fluid inclusion Th data indicate that mineralisation temperatures were possibly slightly lower in the stratabound mineralisation than in the associated veins, as would probably be expected as the incoming brines cooled on contact with the lower-temperature host-rocks.

Although models of fluid mixing have been invoked to explain ore precipitation within the main vein system, direct evidence for the mixing of fluids of contrasting salinities during quartz–fluorite–sulphide mineralisation has not been directly proven. By investigating the stratabound mineralisation at the margins of the veins, we have been able to demonstrate the presence of multiple fluids associated with the mineralisation. These fluids are interpreted as low salinity, sodic, groundwaters, probably infiltrated into the system during late Carboniferous/early Permian unroofing, and a high salinity, calcic, metalliferous brine, with notably high Fe contents that, as previously invoked by Cann and Banks (2001), was probably ultimately sourced from the Zechstein Sea, convected through the Palaeozoic basement, the Weardale Granite and/or the Whin Sill, during which time it picked up significant amounts of dissolved metals and fluorine.

Barite mineralisation is paragenetically late within both within the stratabound deposits and the North Pennine Orefield system as a whole, and slightly different conditions appear to have been responsible for its precipitation, including lower temperatures and lower overall salinities.

References

- ALLAN, M M, YARDLEY, B W D, FORBES, L J, SHMULOVICH, K I, BANKS, D A, and SHEPHERD, T J. 2006. Validation of LA-ICP-MS fluid inclusion analysis with synthetic inclusions. *American Mineralogist* Vol. 90, 11–12.
- ARNE, D C, and KISSIN, S A. 1989. The significance of 'diagenetic crystallization rhythmites' at the Nanisivik Pb-Zn-Ag deposit, Baffin island, Canada. *Mineralium Deposita*, Vol. 24, 230–232.
- BAU, M, ROMER, R L, LÜDERS, V, and DULSKI, P. 2003. Tracing element sources of hydrothermal mineral deposits: REE and Y distribution and Sr-Nd-Pb isotopes in fluorite from MVT deposits in the Pennine Orefield, England. *Mineralium Deposita*, Vol. 38, 992–1008.
- BOLES, J R, and FRANKS, S G. 1979. Clay diagenesis in Wilcox sandstones of Southwest Texas; implications of smectite diagenesis on sandstone cementation. *Journal of Sedimentary Petrology*, Vol. 49, 55–70.
- BONI, M, PARENTE, G, BECHSTADT, T, DE VIVO, B, and IANNACE, A. 2000. Hydrothermal dolomites in SW Sardinia (Italy): evidence for a widespread late-Variscan fluid flow event. *Sedimentary Geology*, Vol. 131, 181–200.
- BRUCKSCHEN, P, and VEIZER, J. 1997. Oxygen and carbon isotopic composition of Dinantian brachiopods: Paleoenvironmental implications for the Lower Carboniferous of western Europe. *Palaeogeography, Palaeoclimatology, Palaeoecology*, Vol. 132, 243–264.
- CANN, J R, and BANKS, D A. 2001. Constraints on the genesis of the mineralization of the Alston Block, Northern Pennine Orefield, northern England. *Proceedings of the Yorkshire Geological Society*, Vol. 53, 187–196.
- CHOQUETTE, P W, and JAMES, N P. 1987. Diagenesis 12. Diagenesis in limestones 3. The deep burial environment. *Geoscience Canada*, Vol. 14, 3–35.
- CHRISTOULA, M. 1993. Fluid Inclusion Geochemistry of Selected Epigenetic, Low Temperature Mineralization in the UK. Unpublished PhD Thesis, Imperial College of Science and Technology, University of London.
- CORBELLA, M, AYORA, C, and CARDELLACH, E. 2004. Hydrothermal mixing, carbonate dissolution and sulfide precipitation in Mississippi Valley-type deposits. *Mineralium Deposita*, Vol. 39, 344–357.
- CROWLEY, S F, BOTTRELL, S H, MCCARTHY, M D B, WARD, J, and YOUNG, B. 1997. Delta S-34 of lower Carboniferous anhydrite, Cumbria and its implications for barite mineralization in northern Pennines. *Journal of the Geological Society London*, Vol. 154, 597–600.
- DAVISON, J M, INESON, P R, and MITCHELL, J G. 1992. Potassium-argon isotope age determinations from the metasomatic alteration of the Great Limestone, Northern Pennine Orefield. *Proceedings of the Yorkshire Geological Society*, Vol. 49, 71–74.
- DUNHAM, K C. 1948. Geology of the Northern Pennine Orefield Volume 1 Tyne to Stainmore, First Edition. *Memoir of the Geological Survey of Great Britain*.
- DUNHAM, K C. 1990. Geology of the Northern Pennine Orefield. Volume 1: Tyne to Stainmore. *Economic Memoir Covering the Areas of 1:50 000 and One-inch Geological Sheets 19 and 25 and Parts of 13, 24, 26, 31, 32 (England and Wales)*. (London: HMSO, for the British Geological Survey.)
- DUNHAM, K C, DUNHAM, A C, HODGE, B L, and JOHNSON, G A L. 1965. Granite beneath Viséan sediments with mineralization at Rookhope, northern Pennines. *Journal of the Geological Society of London*, Vol. 121, 383–417.
- DUNHAM, K C, FITCH, F J, INESON, P R, MILLER, J A, and MITCHELL, J G. 1968. The geochronological significance of argon-40/argon-39 age determinations on White Whin from the northern Pennine orfield. *Proceedings of the Royal Society London (Series A: Mathematical and Physical Sciences)*, Vol. 307, 251–266.
- DUNHAM, K C, and WILSON, A A. 1985. Geology of the Northern Pennine Orefield Volume 2 Stainmore to Craven. *Memoir of the Geological Survey of Great Britain*. (London: HMSO.)
- FITCH, F J, and MILLER, J A. 1967. The age of the Whin sill. *Geological Journal*, Vol. 5, 233–250.
- FRANCOIS, R. 1988. A study on the regulation of the concentrations of some trace metals (Rb, Sr, Zn, Pb, Cu, V, Cr, Ni, Mn and Mo) in Saanich Inlet sediments, British Columbia, Canada. *Marine Geology*, Vol. 83, 285–308.
- FRIEDMAN, I, and O'NEIL, J R. 1977. Compilation of stable isotope fractionation factors of geochemical interest. *United States Geological Survey, Professional Paper*, 440-KK.
- GILG, H A, STRUCK, U, VENNEMANN, T, and BONI, M. 2003. Phosphoric acid fractionation factors for smithsonite and cerussite between 25 and 72°C. *Geochimica et Cosmochimica Acta*, Vol. 67, 4049–4055.
- GOLDSTEIN, R H. 2001. Fluid inclusions in sedimentary and diagenetic systems. *Lithos*, Vol. 55, 159–193.
- GUNTHER, D, FRISCHKNECHT, R, HEINRICH, C A, and KAHLERT, H J. 1997a. Capabilities of an Argon Fluoride 193 nm excimer laser for laser ablation inductively coupled plasma mass spectrometry microanalysis of geological materials. *Journal of Analytical and Atomic Spectrometry*, Vol. 12, 939–944.
- GUNTHER, D, FRISCHKNECHT, R, MUSCHENBORN, H J, and HEINRICH, C A. 1997b. Direct liquid ablation: a new calibration strategy for laser ablation ICP-MS microanalysis of solids and liquids. *Fresenius Journal of Analytical Chemistry*, Vol. 359, 390–393.
- HOLLIS, C, and WALKDEN, G. 1996. The use of burial diagenetic calcite cements to determine the controls upon hydrocarbon emplacement and mineralization on a carbonate platform, Derbyshire, England. *in Recent advances in Lower Carboniferous geology*. STROGEN, P, SOMERVILLE, I D, JONES, G L L. (editors). *Geological Society of London, Special Publication*, Vol. 107, 35–49.
- INESON, P R. 1968. The petrology and geochemistry of altered quartz-dolerite in the Closehouse Mine area. *Proceedings of the Yorkshire Geological Society*, Vol. 36, 373–384.
- IXER, R A. 1986. The ore mineralogy and paragenesis of the lead-zinc-fluorite-barite orefields of the English Pennines and Mendip Hills. 179–211 in *Mineral Parageneses*. CRAIG, J R (editor). (Athens: Theophrastus.)
- IXER, R A, and VAUGHAN, D J. 1993. Lead-zinc-fluorite-baryte deposits of the Pennines, North Wales and the Mendips. 355–418 in *Mineralization in the British Isles*. PATRICK, R A D, and POLYA, D A (editors). (London: Chapman and Hall.)
- IXER, R A, YOUNG, B, and STANLEY, C J. 1996. Bismuth-bearing assemblages from the Northern Pennine Orefield. *Mineralogical Magazine*, Vol. 60, 317–324.
- LENEHAN, T. 1997. An investigation into thermo-tectonic and maturation histories in north-west Britain. Unpublished PhD Thesis, University of Leeds.
- MCCREA, J. 1950. On the isotopic chemistry of carbonates and palaeo-temperature scale. *Journal of Chemistry Physics*, Vol. 18, 849–857.
- MILODOWSKI, A E, GILLESPIE, M R, NADEN, J, FORTEY, N J, SHEPHERD, T J, PEARCE, J M, and METCALFE, R. 1998.

- The petrology and paragenesis of fracture mineralization in the Sellafield area, west Cumbria. *Proceedings of the Yorkshire Geological Society*, Vol. 52, 215–241.
- MOORE, G R. 1980. A Chemical and Isotopic Study of Fluid Inclusions from the Northern Pennine Orefield. Unpublished PhD Thesis, University of Durham.
- NADEN, J. 1996. Calcic Brine 1.5: a Microsoft Excel 5.0 Add-in for calculating salinities from microthermometric data in the system NaCl-CaCl₂-H₂O. PACROFI VI Abstracts. University of Wisconsin.
- NIELSEN, P, SWENNEN, R, MUCHEZ, P, and KEPPENS, E. 1998. Origin of Dinantian zebra dolomites south of the Brabant-Wales Massif, Belgium. *Sedimentology*, Vol. 45, 727–743.
- PLANT, J, JONES, D, SMITH, N, and SHEPHERD, T J. 1995. Carboniferous shale basins as sources of Pennine ore fluids: implications for MVT ore deposit formation. 967–970 in *Mineral deposits: their origin to their environmental impacts*. PASAVA, J, KRIBEK, B, and ZAK, K (editors). (Rotterdam: A. A. Balkema.)
- RANKIN, A H, and GRAHAM, M J. 1988. Na, K and Li contents of mineralizing fluids in the Northern Pennine Orefield, England and their genetic significance. *Transactions of the Institution of Mining and Metallurgy (Sect B: Applied Earth Sciences)*, Vol. 97, 99–107.
- REED, C P, and WALLACE, M W. 2004. Zn-Pb mineralisation in the Silvermines district, Ireland: a product of burial diagenesis. *Mineralium Deposita*, Vol. 39, 87–102.
- ROEDDER, E. 1985. Fluid Inclusions. *Mineralogical Society of America reviews in Mineralogy*, Vol. 12, 644pp.
- ROSENBAUM, J, and SHEPPARD, S M F. 1986. An isotopic study of siderites, dolomites and ankerites at high temperatures. *Geochimica et Cosmochimica Acta*, Vol. 50, 1147–1150.
- SAWKINS, F J. 1966. Ore genesis in the North Pennine orfield, in the light of fluid inclusion studies. *Economic Geology*, Vol 61, 385–401.
- SHEPHERD, T J, DARBYSHIRE, D P F, MOORE, G R, and GREENWOOD, D A. 1982. Rare earth element and isotopic geochemistry of the North Pennine ore deposits. 371–377 in *Gites filoniens Pb-Zn-F-Ba de basse temperature du domaine varisque d'Europe et d'Afrique du Nord; III, Etudes geochimiques et modeles genetiques; etudes structurales; Guide de prospection. Symposium Jules Agard*. ANONYMOUS (editor). (Paris: Bureau de Recherches Geologiques et Minieres.)
- SMITH, F W. 1974. Factors governing the development of fluorspar orebodies in the North Pennine Orefield. Unpublished PhD Thesis, University of Durham.
- SOLOMON, M, RAFTER, T A, and DUNHAM, K C. 1971. Sulphur and oxygen isotope studies in the northern Pennines in relation to ore genesis. *Transactions of the Institution of Mining and Metallurgy (Sect B: Applied Earth Sciences)*, Vol. 80, 259–275.
- SOLOMON, M, RAFTER, T A, and DUNHAM, K C. 1972. Sulphur and oxygen isotope studies in the northern Pennines in relation to ore genesis; discussion. *Transactions of the Institution of Mining and Metallurgy (Sect B: Applied Earth Sciences)*, Vol. 81, 172–177.
- TIMOFEEFF, M N, LOWENSTEIN, T K, BRENNAN, S T, DEMICCO, R V, ZIMMERMANN, H, HORITA, J, and VON BORSTEL, L E. 2001. Evaluating seawater chemistry from fluid inclusions in halite: Examples from modern marine and nonmarine environments. *Geochimica et Cosmochimica Acta*, Vol. 65, 2293–2300.
- TUCKER, M, and WRIGHT, V P. 1990. *Carbonate Sedimentology*. (Blackwell Scientific Publications.)
- VAUGHAN, D J, and IXER, R A. 1980. Studies of sulphide mineralogy of North Pennine ores and its contribution to genetic models. *Transactions of the Institution of Mining and Metallurgy (Sect B: Applied Earth Sciences)*, Vol. 89, 99–109.
- WALLACE, M W, BOTH, R A, RUANO, S M, FENOLL, H A P, and LEES, T. 1994. Zebra textures from carbonate-hosted sulfide deposits; sheet cavity networks produced by fracture and solution enlargement. *Economic Geology*, Vol. 89, 1183–1191.
- WARREN, E, SMALLEY, P, and HOWARTH, R. 1994. Part 4: Compositional variations of North Sea formation waters. 119–206 in *North Sea Formation Waters Atlas*. WARREN, E, and SMALLEY, P (editors). (London: Blackwell Geological Society of London.)
- YOUNG, B, STYLES, M T, and BERRIDGE, N G. 1985. Niccolite-magnetite mineralization from Upper Teesdale, North Pennines. *Mineralogical Magazine*, Vol. 49, 555–559.